Electronic Supplementary Material (ESI) for Nanoscale.

Supporting Information

Magnetite-binding proteins from the magnetotactic bacterium *Desulfamplus magnetovallimortis* BW-1

Anna Pohl,[ab] *Sarah A. E. Young,*[ab] *Tara C. Schmitz,*[a] *Daniel Farhadi,*[a] *Raz Zarivach,*[c] *Damien Faivre*[bd,†] *Kerstin G. Blank*[a,†]

[a]Max Planck Institute of Colloids and Interfaces, Mechano(bio)chemistry, Am Mühlenberg 1, 14476 Potsdam, Germany

[b]Max Planck Institute of Colloids and Interfaces, Department of Biomaterials, Am Mühlenberg 1, 14476 Potsdam, Germany

[c]Department of Life Sciences, The National Institute for Biotechnology in the Negev and Ilse Katz Institute for Nanoscale Science and Technology, Ben-Gurion University of the Negev, Beer Sheva 8410501, Israel

[d]Aix-Marseille Université, CEA, CNRS, BIAM, 13108 Saint Paul lez Durance, France

[†]corresponding authors:

Damien.Faivre@cea.fr

Kerstin.Blank@mpikg.mpg.de

Table of contents

1. Bioinformatics analysis and 3D structure prediction

The amino acid sequences and predicted tertiary structures of Mad1 to Mad11 from *Desulfamplus magnetovallimortis* strain BW-1 are shown below (Fig. S1-S11). All proteins were screened for signal peptides with SignalP v5.0.[1] For Mad5 a signal peptide was predicted; however, with a low probability of only 0.19. Transmembrane regions were identified using TMHMM v2.0.[2] Transmembrane helices were excluded when choosing sequences to be screened for magnetite binding. The structures of Mad proteins are not yet determined. Tertiary structure prediction was used as an additional guide to select sequences for screening. Structure prediction was performed with RaptorX[3] and I-TASSER.[4] For each Mad protein, the highest ranked structure from each prediction is shown. All images were generated with PyMOL (The PyMOL Molecular Graphics System, version v1.8.6.0, Schrödinger, LLC).

```
MKTKICMLPI NKMALKRIKK AAFKVAVILI LSGLLSLIDL PLITKKRPGL   50
ARTAGRAVYY DPTIKDIITN DCGRCHSGPS RNLMDYDNLK AYAESGMLAA  100
MVQGSMSRFA GGDQGTILEW INAGTPEKPA ANQGNVQNNG NTNNNTSKNG  150
VNTAINANFF NGLHHLGGGK GGGGGATQPY VPDVPVNGIT YENTIQYVLA  200
KDCLRCHSGH FRNLTTYDNV SIYVKNGLLK TLVQRGGAMH RFALRDSRWI  250
VAWIENGAPR K                                            261
```

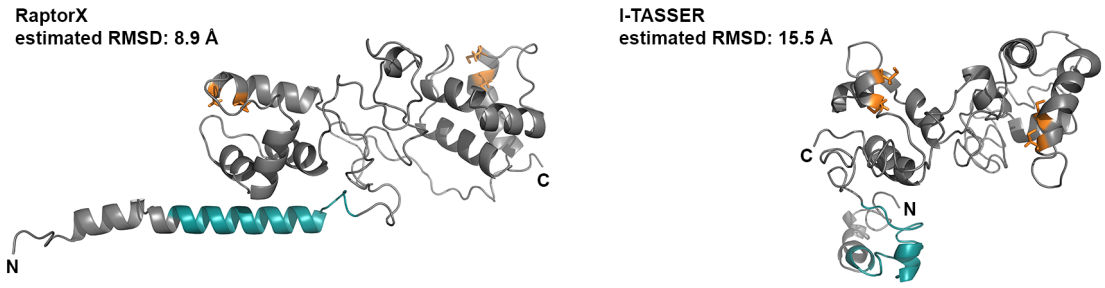

Figure S1. Protein sequence and structure prediction of **Mad1** (accession code: CCO06670). Mad1 contains one predicted transmembrane helix (cyan) as well as four Cys residues (orange). The Cys residues form two magnetochrome CXXCH motifs.[5] As Mad1 has already been assigned as a putative redox protein, it was not included in the screen for magnetite-binding proteins.

MSHIKKTYDI ALFGRGSLKH RVFFVGILVI IGAIYAGKSD YNLATGSGNL 50
CMVLFLAANV YFPAKYIRLK YAIKDVQLQF NRLLVWHIWL NTSSFLVACI 100
HCYVSLWSNR WLMAALFMMG WLTFGGFLMF LKFQPGKVKK GIYLLHTQQV 150
VFFLMIFAML KGHYVI 166

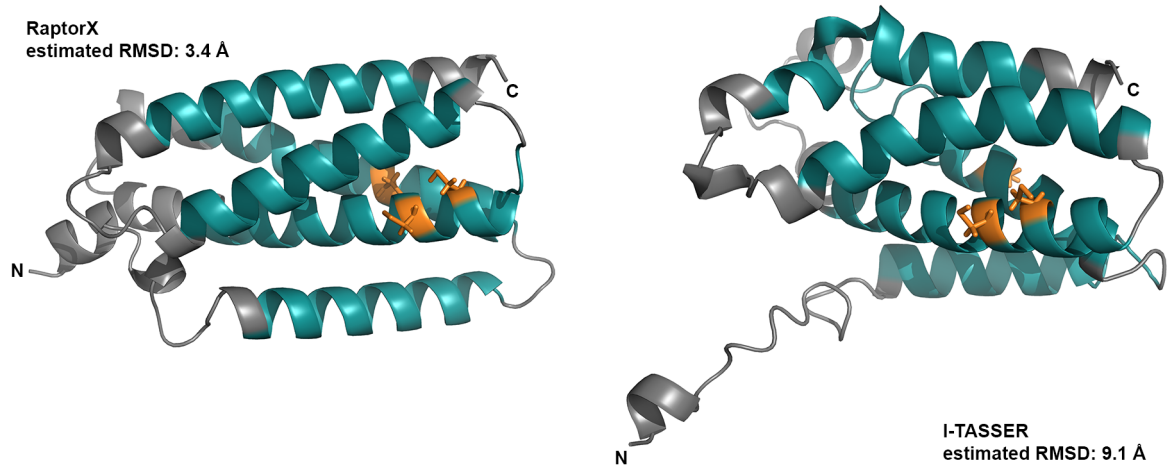

Figure S2. Protein sequence and structure prediction of **Mad2** (accession code: CCO06674). Mad2 contains five predicted transmembrane helices (cyan) and three Cys residues (orange). Due to its high content in transmembrane helices, Mad2 was not included in the screen for magnetite-binding proteins. Structure prediction with I-TASSER suggests that this protein may possess a heme binding site, similar to a hexameric tyrosine-coordinated heme protein (e.g. pdb 2oyy).

MFILRIIGLI LIVTIIIFAF FLVKGATEIE MEIMEEEIMK DHEKAGEN 48

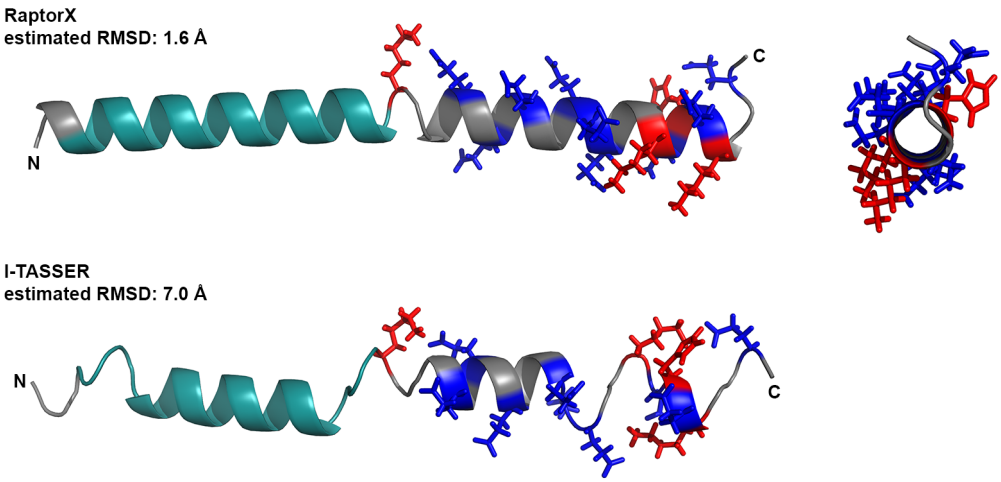

Figure S3. Protein sequence and structure prediction of **Mad3** (accession code: CCO06675). Mad3 contains one predicted transmembrane helix (cyan) and is free of Cys residues. The C-terminal helix is rich in **acidic** (Asp, Glu) and **basic** (Arg, His, Lys) residues. In particular Glu is known to interact with magnetite. This Glu-rich helix (residues 24-48 in bold) was included in our screen.

MIEDYFNINI KR **LLYFAGAI IMAASVTTLL YWFLYGFDTW KNSMNTASDL** 50
MLAAAPGG 58

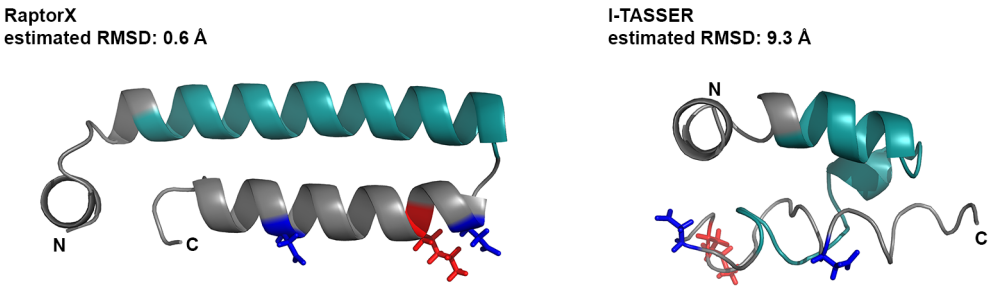

Figure S4. Protein sequence and structure prediction of **Mad4** (accession code: CCO06682). Mad4 contains one predicted transmembrane helix (**cyan**) and is free of Cys residues. Structure prediction with RaptorX suggests that this small protein may fold into helix hairpin, which is incompatible with the presence of an N-terminal transmembrane helix. The structure predicted with I-TASSER is also not compatible with the predicted transmembrane helix. The C-terminal region was included in our screen (residues 46-58 shown in bold). **Acidic** (Asp, Glu) and **basic** (Arg, His, Lys) residues in this region are highlighted.

MGMMMQAAAT APAFQPAYQG NINNTTPAGQ FVCPVHGAAG MPHFDSAGNP 50
ICPFGDQIMQ FHSIGGNIMG SPYNGNTGNA ARGIQSLPGT YGTAVPYGSG 100
VSPNRYTLAA GG 112

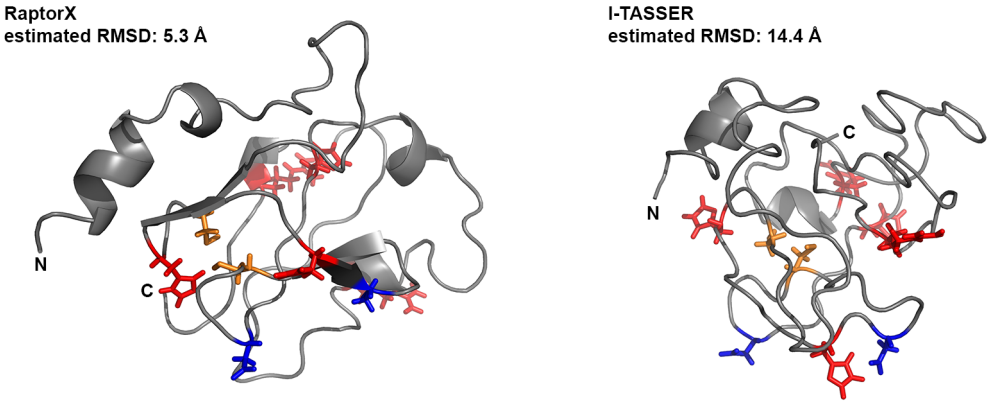

Figure S5. Protein sequence and structure prediction of **Mad5** (accession code: CCO06683). Mad5 is free of predicted transmembrane helices and contains two Cys residues (**orange**). The full-length protein was included in our screen, omitting the N-terminal Met. The putative signal peptide was not considered because of its low probability of only 0.19. **Acidic** (Asp, Glu) and **basic** (Arg, His, Lys) residues are highlighted.

MELTRIRQLM QLAGTVLSNS YIGTIFTKNI STGPLKGVCV PFLNCYACPS 50
AVFSCPIGTL QHFAAIRAIP YYLIGFIAVV GLTVGRMACG WLCPFGFLQD 100
MMHKIPSPKM EIPGTLRYVK YLVLLLLVIV LPYLTAEMTF SILCPAGTLT 150
AGLPWAIWNP VNPQTGLPFF PDGQGAIFFI SLFILIVFLV FFILTKRPFC 200
RIACPMGALL AFFNKYSMVQ LKVSSKCDGC NICRDLCPVD INISMEEDSG 250
ECIRCLECTR CAHVKLSTPF SSDIKAQKLF RKAKLKGQRV KG 292

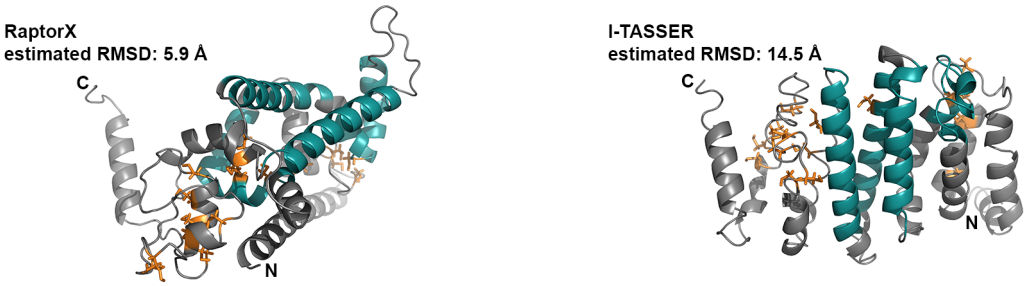

Figure S6. Protein sequence and structure prediction of **Mad6** (accession code: CCO06684). Mad6 contains four predicted transmembrane helices (cyan) and a large number of Cys residues (orange). It shows homology to 4Fe-4S ferredoxin iron-sulfur binding proteins and was therefore not included in our screen.

MDIKSKCASC EIQGYCPELC KAHIRKLATG KQDKSECTRY SPSLMKYGKT 50
AAVGAGVGLA VATGSMAAIP SVTLKTLFAH VTAHVAAVKA GAGAGGGITG 100
AGINIFRQKR REQPKPAKKR RHLYYPLVLN GGTANDK 137

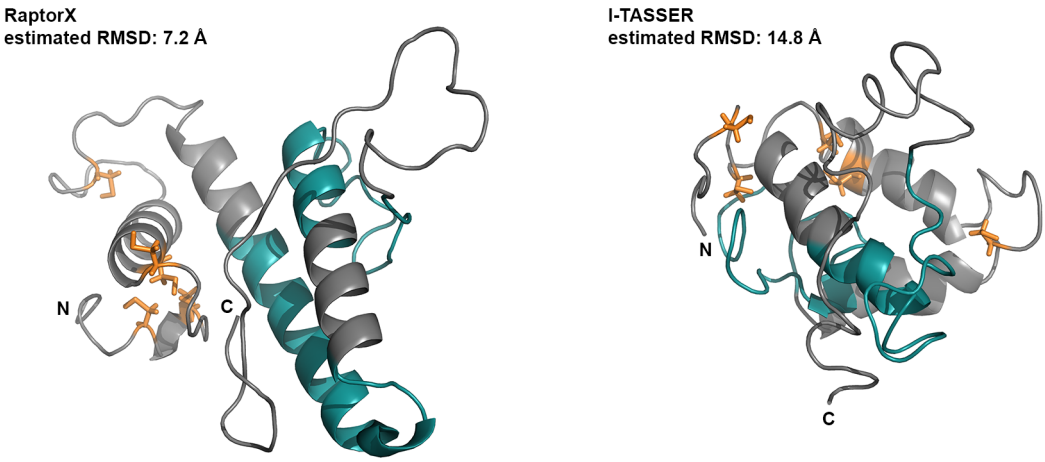

Figure S7. Protein sequence and structure prediction of **Mad7** (accession code: CCO06689). Mad7 contains two predicted transmembrane helices (cyan) and five Cys residues (orange). The protein was not included in our screen because of its relatively high number of Cys residues.

```
MTNREIRDDN LKTESQARPD DWKTEPEYDP YDDYEDHDHR TAQNSHVKYD   50
DVDSIDNDFG FSDLMQVGSK VLIGGGIGLL GGIATIAVAA SAAEVVITGV  100
VTKIAGVVGG AAGLSMGISS YKKRKYH                           127
```

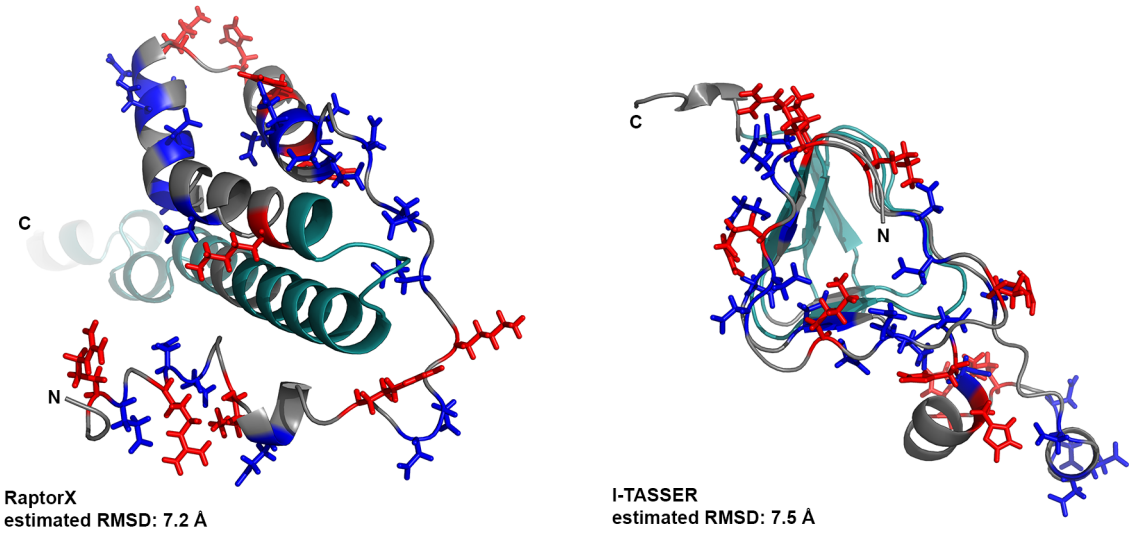

Figure S8. Protein sequence and structure prediction of **Mad8** (accession code: CCO06690). Mad8 contains two predicted transmembrane helices (**cyan**). Structure prediction with I-TASSER, however, revealed a possible C-terminal hexapeptide repeat structure. The I-TASSER results further suggest that this protein may be functionally related to acetyl transferases. Despite this prediction result, the N-terminal region (residues 2-70) was included in our screen as it contains a large number of **acidic** (Asp, Glu) and **basic** (Arg, His, Lys) amino acids. The N-terminal Met was omitted.

```
MSYTIVTDAC IACGACAKKC PENAIFGKVK VGFEIDPFVC MDCGNCFDTC   50
KRGAIEDPFG DRSAVRNRKQ ENTKAVIDSE ICAGCKICFM NCPQEAISII  100
KKGLFTGSFC QVDSSLCVGC GTCTEYCITG AVSLEKFV               138
```

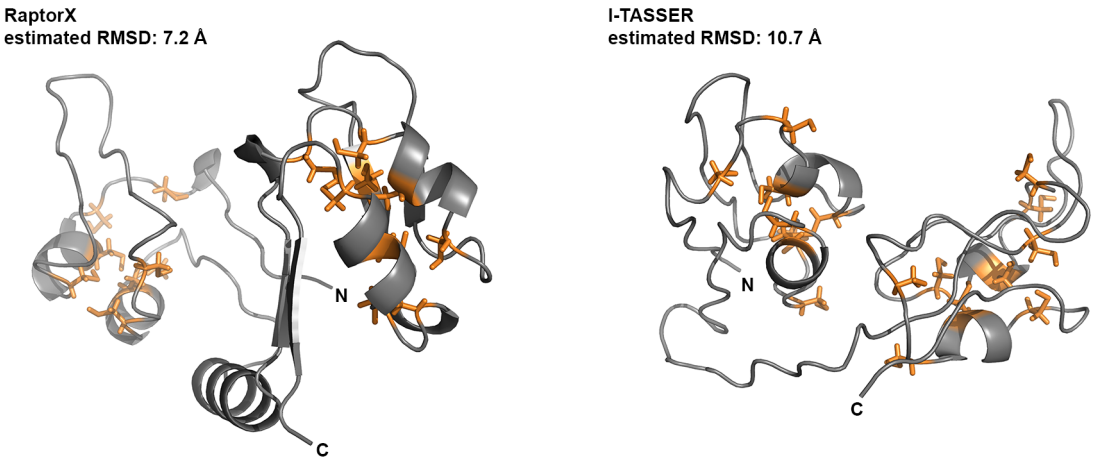

Figure S9. Protein sequence and structure prediction of **Mad9** (accession code: CCO06691). Mad9 contains no transmembrane helices and a total number of 17 Cys residues (**orange**). Mad9 shows homology to 4Fe-4S ferredoxin iron-sulfur binding proteins and was not included in our screen.

MGRGIRYTMY NLGDIFVDKL ESMWNSTKIS TKGIRLTHNI RKLRSIKEEQ 50
ERKLSGRVLE LRESYPELEI FKDDELSKLF SEIDAINREL DSYIEERDEI 100
LYPTGRSVCS QCA 113

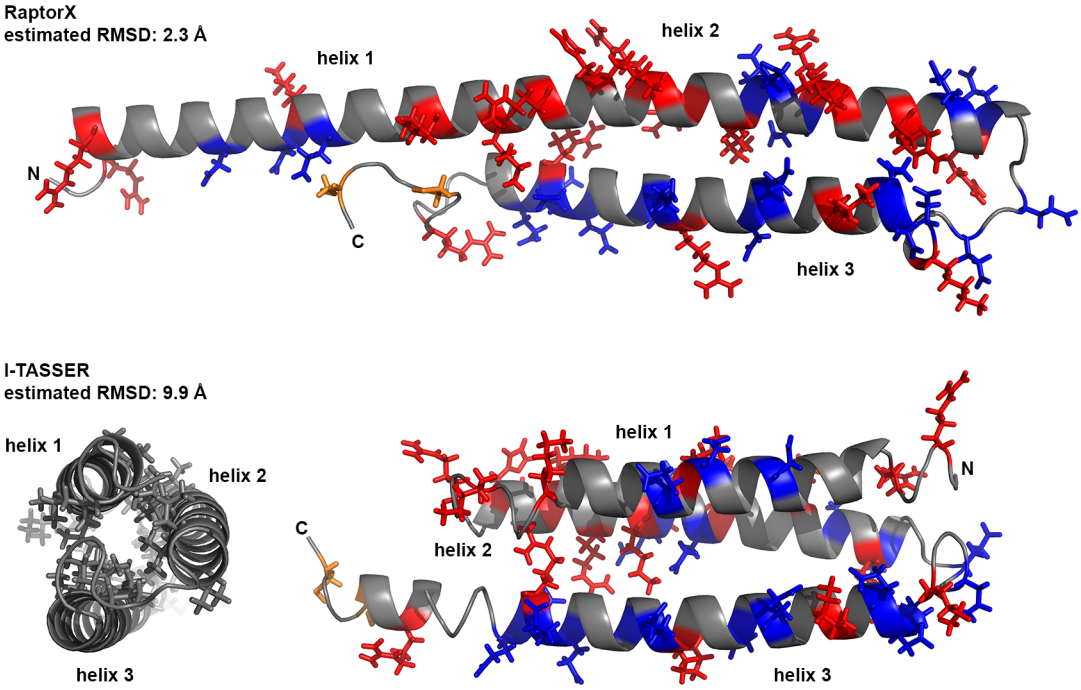

Figure S10. Protein sequence and structure prediction of **Mad10** (accession code: CCO06692). Mad10 contains no predicted transmembrane helices and only two C-terminal Cys residues (orange). The helices are amphiphilic and are predicted to form dimeric or trimeric coiled coil-like superhelical structures. The hydrophobic side chains (Ile, Leu and Val), located at the predicted trimeric interface, are shown in the front view of the corresponding I-TASSER prediction (grey). Mad10 was included in our screen as it contains a large number of **acidic** (Asp, Glu) and **basic** (Arg, His, Lys) residues. The I-TASSER prediction of possible ligands further suggests that Mad10 may bind heme, similar to bacterioferritin (e.g. pdb 3uoi, 2vxi and 1jgc). Most importantly, helix 3 (residues 74-99) was already shown to bind to magnetite.[6] In addition to the full-length protein, a truncated version lacking the last five amino acids (CSQCA) was used for the screen. In both proteins, the N-terminal Met was omitted.

```
MDDNHRGKFY SRMTYSISAV EYLGLVSKSL MVKGNRSLKK FGWAAIDGVT    50
APFARIKKRS VSNKKLYSTP YDILHLDHPA LRNGNKLSDL EASISRLEER   100
LAQLEKRGIA ISGNHQKQPE TAEKEKKEIN EEKRAILRML VNENKQLRKM   150
AEN                                                      153
```

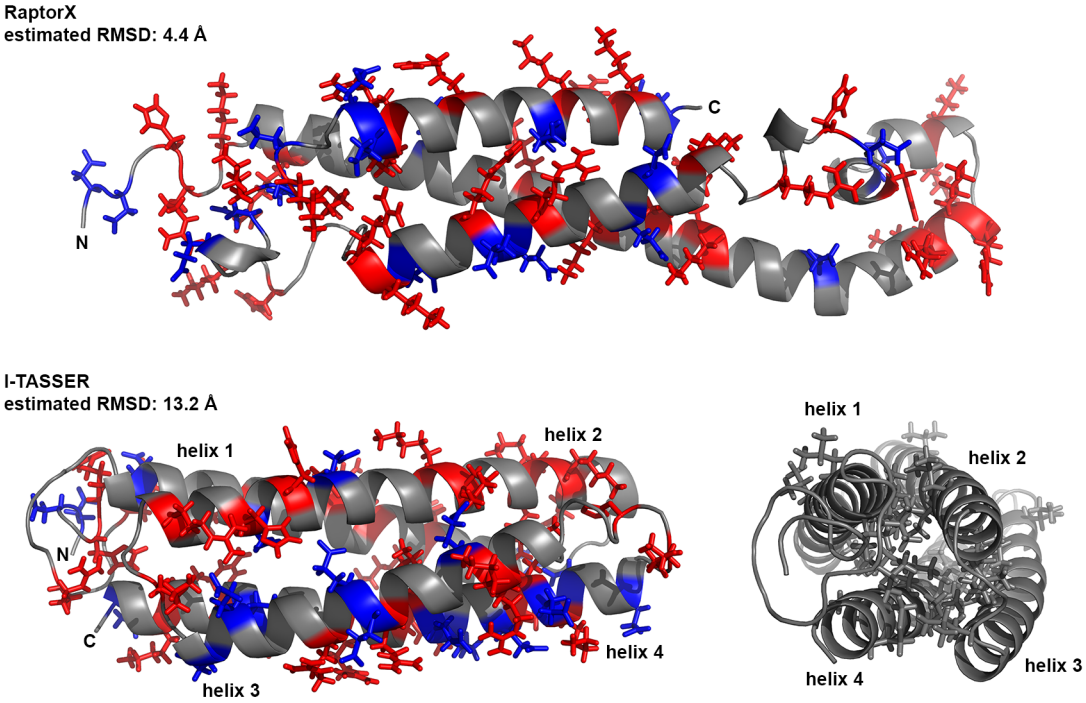

Figure S11. Protein sequence and structure prediction of **Mad11** (accession code: CCO06693). Mad11 contains no predicted transmembrane helices and no Cys residues. The helices are amphiphilic and are predicted to form trimeric or tetrameric coiled coil-like superhelical structures. The hydrophobic side chains (Ile, Leu and Val), located at the predicted tetrameric interface, are shown in the front view of the respective I-TASSER prediction (grey). The I-TASSER prediction of possible ligands further suggests that Mad11 may possess an oxygen-binding di-iron site, with similarities to hemerythrin, which is involved in oxygen storage and transport (e.g. pdb 2avk and 1hmo). Mad11 was included in our screen as it contains a large number of **acidic** (Asp, Glu) and **basic** (Arg, His, Lys) residues. The N-terminal Met was omitted.

2. Gene design and cloning

The codon optimized genes were obtained via gene synthesis (Eurofins Genomics) and cloned into the expression vector pET28a (Merck), using standard protocols. The coding regions of the expression plasmids were verified by sequencing. All fusion proteins with superfolder green fluorescent protein[7] (sfGFP) have the same general structure. From N-terminus to C-terminus, the sequences were fused in the following order: sfGFP (amino acids 1-229[8]), linker with enterokinase cleavage site (DDDDK), Mad protein and $(His)_6$ tag. For Mad10, two sfGFP fusion proteins were cloned: the full-length protein and one protein where the last 5 amino acids (CSQCA) were deleted (Mad10trunc). In addition, Mad10trunc was cloned without the sfGFP fusion partner, either carrying an N-terminal or C-terminal $(His)_6$ tag. The protein and DNA sequences of each construct are given below. For both sequences, the region containing the respective Mad protein is highlighted in bold. For the DNA sequences, the restriction sites used for cloning (NcoI and EagI) are underlined.

sfGFP-Mad3-His ($Mad3_{24-48}$)

MGSKGEELFTGVVPILVELDGDVNGHKFSVRGEGEGDATNGKLTLKFICTTGKLPVPWPTLVTTLTYGVQC
FSRYPDHMKQHDFFKSAMPEGYVQERTISFKDDGTYKTRAEVKFEGDTLVNRIELKGIDFKEDGNILGHKL
EYNFNSHNVYITADKQKNGIKANFKIRHNVEDGSVQLADHYQQNTPIGDGPVLLPDNHYLSTQSVLSKDPN
EKRDHMVLLEFVTAAGIGSDDDDKEF**KGATEIEMEIMEEEIMKDHEKAGEN**ASHHHHHH

CCATGGGCAGCAAGGGTGAGGAACTATTCACGGGCGTAGTTCCAATTCTCGTAGAGCTGGACGGGGATGTC
AACGGCCACAAATTTTCTGTGCGCGGGGAGGGGGAGGGGGATGCTACCAACGGCAAATTGACTTTGAAATT
TATCTGCACCACTGGTAAACTGCCTGTGCCTTGGCCGACGTTGGTTACGACCCTGACCTATGGAGTCCAAT
GTTTCTCGCGGTATCCGGATCACATGAAACAGCATGACTTCTTCAAGAGCGCAATGCCCGAGGGTTATGTG
CAAGAGCGCACTATCTCGTTTAAGGACGATGGCACTTATAAAACTCGCGCAGAAGTCAAGTTCGAGGGTGA
TACTTTAGTCAATCGTATAGAACTTAAAGGTATAGACTTCAAGGAAGATGGAAACATCCTGGGCCATAAAT
TAGAATATAATTTTAATAGCCACAATGTATACATTACCGCAGACAAACAAAAAAACGGTATAAAAGCTAAC
TTCAAAATTCGTCATAACGTGGAAGACGGATCGGTACAACTCGCCGACCATTACCAGCAAAACACTCCAAT
AGGTGATGGTCCGGTGCTGCTGCCGGATAACCACTATCTTTCTACTCAAAGTGTCCTAAGTAAAGACCCGA
ACGAAAAAAGAGATCATATGGTATTATTAGAATTTGTGACAGCGGCAGGGATTGGATCCGATGACGACGAT
AAGGAATTC**AAAGGCGCGACCGAGATTGAGATGGAAATCATGGAAGAAGAAATTATGAAAGATCATGAAAA
GGCCGGTGAAAAC**GCTAGCCATCACCATCATCACCACTAACGGCCG

sfGFP-Mad4-His ($Mad4_{46-58}$)

MGSKGEELFTGVVPILVELDGDVNGHKFSVRGEGEGDATNGKLTLKFICTTGKLPVPWPTLVTTLTYGVQC
FSRYPDHMKQHDFFKSAMPEGYVQERTISFKDDGTYKTRAEVKFEGDTLVNRIELKGIDFKEDGNILGHKL
EYNFNSHNVYITADKQKNGIKANFKIRHNVEDGSVQLADHYQQNTPIGDGPVLLPDNHYLSTQSVLSKDPN
EKRDHMVLLEFVTAAGIGSDDDDKEF**GFDTWKNSMNTASDLMLAAAPGG**ASHHHHHH

CCATGGGCAGCAAGGGTGAGGAACTATTCACGGGCGTAGTTCCAATTCTCGTAGAGCTGGACGGGGATGTC
AACGGCCACAAATTTTCTGTGCGCGGGGAGGGGGAGGGGGATGCTACCAACGGCAAATTGACTTTGAAATT
TATCTGCACCACTGGTAAACTGCCTGTGCCTTGGCCGACGTTGGTTACGACCCTGACCTATGGAGTCCAAT
GTTTCTCGCGGTATCCGGATCACATGAAACAGCATGACTTCTTCAAGAGCGCAATGCCCGAGGGTTATGTG
CAAGAGCGCACTATCTCGTTTAAGGACGATGGCACTTATAAAACTCGCGCAGAAGTCAAGTTCGAGGGTGA

TACTTTAGTCAATCGTATAGAACTTAAAGGTATAGACTTCAAGGAAGATGGAAACATCCTGGGCCATAAAT
TAGAATATAATTTTAATAGCCACAATGTATACATTACCGCAGACAAACAAAAAAACGGTATAAAAGCTAAC
TTCAAAATTCGTCATAACGTGGAAGACGGATCGGTACAACTCGCCGACCATTACCAGCAAAACACTCCAAT
AGGTGATGGTCCGGTGCTGCTGCCGGATAACCACTATCTTTCTACTCAAAGTGTCCTAAGTAAAGACCCGA
ACGAAAAAAGAGATCATATGGTATTATTAGAATTTGTGACAGCGGCAGGGATTGGATCCGATGACGACGAT
AAGGAATTC**GGGTTTGACACGTGGAAGAACTCGATGAACACAGCGTCAGATCTGATGTTAGCTGCTGCTCC**
TGGTGGAGCTAGCCATCACCATCATCACCACTAACGGCCG

sfGFP-Mad5-His (Mad5$_{2-112}$)

MGSKGEELFTGVVPILVELDGDVNGHKFSVRGEGEGDATNGKLTLKFICTTGKLPVPWPTLVTTLTYGVQC
FSRYPDHMKQHDFFKSAMPEGYVQERTISFKDDGTYKTRAEVKFEGDTLVNRIELKGIDFKEDGNILGHKL
EYNFNSHNVYITADKQKNGIKANFKIRHNVEDGSVQLADHYQQNTPIGDGPVLLPDNHYLSTQSVLSKDPN
EKRDHMVLLEFVTAAGIGSDDDDKEF**GMMMQAAATAPAFQPAYQGNINNTTPAGQFVCPVHGAAGMPHFDS**
AGNPICPFGDQIMQFHSIGGNIMGSPYNGNTGNAARGIQSLPGTYGTAVPYGSGVSPNRYTLAAGGASHHH
HHH

CCATGGGCAGCAAGGGTGAGGAACTATTCACGGGCGTAGTTCCAATTCTCGTAGAGCTGGACGGGGATGTC
AACGGCCACAAATTTTCTGTGCGCGGGGAGGGGGAGGGGGATGCTACCAACGGCAAATTGACTTTGAAATT
TATCTGCACCACTGGTAAACTGCCTGTGCCTTGGCCGACGTTGGTTACGACCCTGACCTATGGAGTCCAAT
GTTTCTCGCGGTATCCGGATCACATGAAACAGCATGACTTCTTCAAGAGCGCAATGCCCGAGGGTTATGTG
CAAGAGCGCACTATCTCGTTTAAGGACGATGGCACTTATAAAACTCGCGCAGAAGTCAAGTTCGAGGGTGA
TACTTTAGTCAATCGTATAGAACTTAAAGGTATAGACTTCAAGGAAGATGGAAACATCCTGGGCCATAAAT
TAGAATATAATTTTAATAGCCACAATGTATACATTACCGCAGACAAACAAAAAAACGGTATAAAAGCTAAC
TTCAAAATTCGTCATAACGTGGAAGACGGATCGGTACAACTCGCCGACCATTACCAGCAAAACACTCCAAT
AGGTGATGGTCCGGTGCTGCTGCCGGATAACCACTATCTTTCTACTCAAAGTGTCCTAAGTAAAGACCCGA
ACGAAAAAAGAGATCATATGGTATTATTAGAATTTGTGACAGCGGCAGGGATTGGATCCGATGACGACGAT
AAGGAATTC**GGCATGATGATGCAAGCAGCCGCAACCGCTCCCGCATTCCAGCCGGCGTACCAGGGGAACAT**
TAATAATACGACTCCTGCGGGACAATTCGTCTGTCCTGTTCACGGTGCAGCCGGCATGCCACATTTTGACT
CAGCGGGCAATCCAATCTGCCCGTTTGGCGATCAGATTATGCAGTTTCATTCGATTGGTGGCAACATCATG
GGCTCCCCTTACAACGGTAACACAGGTAACGCTGCTCGTGGAATCCAGTCGCTGCCGGGTACGTATGGCAC
CGCGGTGCCGTATGGTTCTGGGGTAAGCCCGAATCGCTATACCCTGGCCGCCGGCGGTGCTAGCCATCACC
ATCATCACCACTAACGGCCG

sfGFP-Mad8-His (Mad8$_{2-70}$)

MGSKGEELFTGVVPILVELDGDVNGHKFSVRGEGEGDATNGKLTLKFICTTGKLPVPWPTLVTTLTYGVQC
FSRYPDHMKQHDFFKSAMPEGYVQERTISFKDDGTYKTRAEVKFEGDTLVNRIELKGIDFKEDGNILGHKL
EYNFNSHNVYITADKQKNGIKANFKIRHNVEDGSVQLADHYQQNTPIGDGPVLLPDNHYLSTQSVLSKDPN
EKRDHMVLLEFVTAAGIGSDDDDKEF**TNREIRDDNLKTESQARPDDWKTEPEYDPYDDYEDHDHRTAQNSH**
VKYDDVDSIDNDFGFSDLMQVGSKASHHHHHH

CCATGGGCAGCAAGGGTGAGGAACTATTCACGGGCGTAGTTCCAATTCTCGTAGAGCTGGACGGGGATGTC
AACGGCCACAAATTTTCTGTGCGCGGGGAGGGGGAGGGGGATGCTACCAACGGCAAATTGACTTTGAAATT
TATCTGCACCACTGGTAAACTGCCTGTGCCTTGGCCGACGTTGGTTACGACCCTGACCTATGGAGTCCAAT
GTTTCTCGCGGTATCCGGATCACATGAAACAGCATGACTTCTTCAAGAGCGCAATGCCCGAGGGTTATGTG
CAAGAGCGCACTATCTCGTTTAAGGACGATGGCACTTATAAAACTCGCGCAGAAGTCAAGTTCGAGGGTGA
TACTTTAGTCAATCGTATAGAACTTAAAGGTATAGACTTCAAGGAAGATGGAAACATCCTGGGCCATAAAT
TAGAATATAATTTTAATAGCCACAATGTATACATTACCGCAGACAAACAAAAAAACGGTATAAAAGCTAAC
TTCAAAATTCGTCATAACGTGGAAGACGGATCGGTACAACTCGCCGACCATTACCAGCAAAACACTCCAAT
AGGTGATGGTCCGGTGCTGCTGCCGGATAACCACTATCTTTCTACTCAAAGTGTCCTAAGTAAAGACCCGA
ACGAAAAAAGAGATCATATGGTATTATTAGAATTTGTGACAGCGGCAGGGATTGGATCCGATGACGACGAT
AAGGAATTC**ACGAATCGCGAGATTCGCGATGATAACCTGAAAACCGAATCTCAGGCGCGTCCAGATGACTG**
GAAAACCGAACCGGAATACGATCCGTATGACGATTACGAGGATCACGATCATCGTACTGCCCAGAATAGCC
ATGTGAAGTATGACGACGTTGATTCCATCGACAACGATTTCGGCTTTTCGGACTTAATGCAAGTCGGTAGT
AAAGCTAGCCATCACCATCATCACCACTAACGGCCG

sfGFP-Mad10trunc-His (Mad10$_{2-108}$)

MGSKGEELFTGVVPILVELDGDVNGHKFSVRGEGEGDATNGKLTLKFICTTGKLPVPWPTLVTTLTYGVQC
FSRYPDHMKQHDFFKSAMPEGYVQERTISFKDDGTYKTRAEVKFEGDTLVNRIELKGIDFKEDGNILGHKL
EYNFNSHNVYITADKQKNGIKANFKIRHNVEDGSVQLADHYQQNTPIGDGPVLLPDNHYLSTQSVLSKDPN
EKRDHMVLLEFVTAAGIGSDDDDKEF**GRGIRYTMYNLGDIFVDKLESMWNSTKISTKGIRLTHNIRKLRSI**
KEEQERKLSGRVLELRESYPELEIFKDDELSKLFSEIDAINRELDSYIEERDEILYPTGRSVASHHHHHH

CCATGGGCAGCAAGGGTGAGGAACTATTCACGGGCGTAGTTCCAATTCTCGTAGAGCTGGACGGGGATGTC
AACGGCCACAAATTTTCTGTGCGCGGGGAGGGGGAGGGGGATGCTACCAACGGCAAATTGACTTTGAAATT
TATCTGCACCACTGGTAAACTGCCTGTGCCTTGGCCGACGTTGGTTACGACCCTGACCTATGGAGTCCAAT
GTTTCTCGCGGTATCCGGATCACATGAAACAGCATGACTTCTTCAAGAGCGCAATGCCCGAGGGTTATGTG
CAAGAGCGCACTATCTCGTTTAAGGACGATGGCACTTATAAAACTCGCGCAGAAGTCAAGTTCGAGGGTGA
TACTTTAGTCAATCGTATAGAACTTAAAGGTATAGACTTCAAGGAAGATGGAAACATCCTGGGCCATAAAT
TAGAATATAATTTTAATAGCCACAATGTATACATTACCGCAGACAAACAAAAAAACGGTATAAAAGCTAAC
TTCAAAATTCGTCATAACGTGGAAGACGGATCGGTACAACTCGCCGACCATTACCAGCAAAACACTCCAAT
AGGTGATGGTCCGGTGCTGCTGCCGGATAACCACTATCTTTCTACTCAAAGTGTCCTAAGTAAAGACCCGA
ACGAAAAAAGAGATCATATGGTATTATTAGAATTTGTGACAGCGGCAGGGATTGGATCCGATGACGACGAT
AAGGAATTC**GGACGCGGTATTCGATATACGATGTACAATCTTGGCGATATCTTCGTTGACAAGCTGGAATC**
CATGTGGAACTCGACTAAAATCAGCACAAAAGGTATTCGCCTGACCCATAATATCCGCAAATTACGGTCAA
TTAAAGAGGAGCAGGAGCGCAAGCTCAGTGGGCGTGTCCTAGAGTTACGTGAATCGTATCCAGAATTGGAA
ATCTTTAAAGACGACGAACTGTCTAAACTGTTTAGTGAAATTGATGCGATAAACCGCGAACTGGATAGCTA
TATCGAAGAACGTGATGAAATTCTGTACCCGACCGGTCGTTCTGTGGCTAGCCATCACCATCATCACCACT
AACGGCCG

sfGFP-Mad10-His (Mad10$_{2-113}$)

MGSKGEELFTGVVPILVELDGDVNGHKFSVRGEGEGDATNGKLTLKFICTTGKLPVPWPTLVTTLTYGVQC
FSRYPDHMKQHDFFKSAMPEGYVQERTISFKDDGTYKTRAEVKFEGDTLVNRIELKGIDFKEDGNILGHKL
EYNFNSHNVYITADKQKNGIKANFKIRHNVEDGSVQLADHYQQNTPIGDGPVLLPDNHYLSTQSVLSKDPN
EKRDHMVLLEFVTAAGIGSDDDDKEF**GRGIRYTMYNLGDIFVDKLESMWNSTKISTKGIRLTHNIRKLRSI**
KEEQERKLSGRVLELRESYPELEIFKDDELSKLFSEIDAINRELDSYIEERDEILYPTGRSVCSQCAASHH
HHHH

CCATGGGCAGCAAGGGTGAGGAACTATTCACGGGCGTAGTTCCAATTCTCGTAGAGCTGGACGGGGATGTC
AACGGCCACAAATTTTCTGTGCGCGGGGAGGGGGAGGGGGATGCTACCAACGGCAAATTGACTTTGAAATT
TATCTGCACCACTGGTAAACTGCCTGTGCCTTGGCCGACGTTGGTTACGACCCTGACCTATGGAGTCCAAT
GTTTCTCGCGGTATCCGGATCACATGAAACAGCATGACTTCTTCAAGAGCGCAATGCCCGAGGGTTATGTG
CAAGAGCGCACTATCTCGTTTAAGGACGATGGCACTTATAAAACTCGCGCAGAAGTCAAGTTCGAGGGTGA
TACTTTAGTCAATCGTATAGAACTTAAAGGTATAGACTTCAAGGAAGATGGAAACATCCTGGGCCATAAAT
TAGAATATAATTTTAATAGCCACAATGTATACATTACCGCAGACAAACAAAAAAACGGTATAAAAGCTAAC
TTCAAAATTCGTCATAACGTGGAAGACGGATCGGTACAACTCGCCGACCATTACCAGCAAAACACTCCAAT
AGGTGATGGTCCGGTGCTGCTGCCGGATAACCACTATCTTTCTACTCAAAGTGTCCTAAGTAAAGACCCGA
ACGAAAAAAGAGATCATATGGTATTATTAGAATTTGTGACAGCGGCAGGGATTGGATCCGATGACGACGAT
AAGGAATTC**GGGCGTGGGATTCGGTATACGATGTACAACCTCGGAGATATCTTCGTCGATAAGCTAGAGTC**
CATGTGGAATAGCACTAAAATCTCGACCAAAGGTATTCGACTCACACATAACATTAGGAAACTGCGTAGTA
TAAAAGAAGAACAGGAGCGCAAATTGTCCGGCAGGGTTTTGGAATTACGCGAGTCGTACCCGGAGCTGGAA
ATTTTTAAGGATGATGAACTGTCGAAACTGTTCTCGGAAATAGACGCCATCAATCGTGAACTGGACAGCTA
TATCGAAGAACGCGACGAAATTCTGTATCCAACTGGGCGCAGTGTGTGCAGTCAATGTGCGGCTAGCCATC
ACCATCATCACCACTAACGGCCG

His-Mad10trunc (Mad10$_{2-109}$)

MGHHHHHHEF**GRGIRYTMYNLGDIFVDKLESMWNSTKISTKGIRLTHNIRKLRSIKEEQERKLSGRVLELR**
ESYPELEIFKDDELSKLFSEIDAINRELDSYIEERDEILYPTGRSVC

CCATGGGCCATCACCATCATCACCATGAATTC**GGACGCGGTATTCGATATACGATGTACAATCTTGGCGAT**
ATCTTCGTTGACAAGCTGGAATCCATGTGGAACTCGACTAAAATCAGCACAAAAGGTATTCGCCTGACCCA
TAATATCCGCAAATTACGGTCAATTAAAGAGGAGCAGGAGCGCAAGCTCAGTGGGCGTGTCCTAGAGTTAC
GTGAATCGTATCCAGAATTGGAAATCTTTAAAGACGACGAACTGTCTAAACTGTTTAGTGAAATTGATGCG
ATAAACCGCGAACTGGATAGCTATATCGAAGAACGTGATGAAATTCTGTACCCGACCGGTCGTTCTGTGTG
CTAACGGCCG

Mad10trunc-His (Mad10$_{1-108}$)

MGRGIRYTMYNLGDIFVDKLESMWNSTKISTKGIRLTHNIRKLRSIKEEQERKLSGRVLELRESYPELEIF
KDDELSKLFSEIDAINRELDSYIEERDEILYPTGRSVASHHHHHHGGC

CCATG**GGACGCGGTATTCGATATACGATGTACAATCTTGGCGATATCTTCGTTGACAAGCTGGAATCC**
ATGTGGAACTCGACTAAAATCAGCACAAAAGGTATTCGCCTGACCCATAATATCCGCAAATTACGGTC
AATTAAAGAGGAGCAGGAGCGCAAGCTCAGTGGGCGTGTCCTAGAGTTACGTGAATCGTATCCAGAAT
TGGAAATCTTTAAAGACGACGAACTGTCTAAACTGTTTAGTGAAATTGATGCGATAAACCGCGAACTG
GATAGCTATATCGAAGAACGTGATGAAATTCTGTACCCGACCGGTCGTTCTGTGGCTAGCCATCACCA
TCATCACCACGGGGGCTGCTAACGGCCG

sfGFP-Mad11-His (Mad11$_{2-153}$)

MGSKGEELFTGVVPILVELDGDVNGHKFSVRGEGEGDATNGKLTLKFICTTGKLPVPWPTLVTTLTYGVQC
FSRYPDHMKQHDFFKSAMPEGYVQERTISFKDDGTYKTRAEVKFEGDTLVNRIELKGIDFKEDGNILGHKL
EYNFNSHNVYITADKQKNGIKANFKIRHNVEDGSVQLADHYQQNTPIGDGPVLLPDNHYLSTQSVLSKDPN
EKRDHMVLLEFVTAAGIGSDDDDKEF**DDNHRGKFYSRMTYSISAVEYLGLVSKSLMVKGNRSLKKFGWAAI**
DGVTAPFARIKKRSVSNKKLYSTPYDILHLDHPALRNGNKLSDLEASISRLEERLAQLEKRGIAISGNHQK
QPETAEKEKKEINEEKRAILRMLVNENKQLRKMAENASHHHHHH

CCATGGGCAGCAAGGGTGAGGAACTATTCACGGGCGTAGTTCCAATTCTCGTAGAGCTGGACGGGGATGTC
AACGGCCACAAATTTTCTGTGCGCGGGGAGGGGGAGGGGGATGCTACCAACGGCAAATTGACTTTGAAATT
TATCTGCACCACTGGTAAACTGCCTGTGCCTTGGCCGACGTTGGTTACGACCCTGACCTATGGAGTCCAAT
GTTTCTCGCGGTATCCGGATCACATGAAACAGCATGACTTCTTCAAGAGCGCAATGCCCGAGGGTTATGTG
CAAGAGCGCACTATCTCGTTTAAGGACGATGGCACTTATAAAACTCGCGCAGAAGTCAAGTTCGAGGGTGA
TACTTTAGTCAATCGTATAGAACTTAAAGGTATAGACTTCAAGGAAGATGGAAACATCCTGGGCCATAAAT
TAGAATATAATTTTAATAGCCACAATGTATACATTACCGCAGACAAACAAAAAAACGGTATAAAAGCTAAC
TTCAAAATTCGTCATAACGTGGAAGACGGATCGGTACAACTCGCCGACCATTACCAGCAAAACACTCCAAT
AGGTGATGGTCCGGTGCTGCTGCCGGATAACCACTATCTTTCTACTCAAAGTGTCCTAAGTAAAGACCCGA
ACGAAAAAAGAGATCATATGGTATTATTAGAATTTGTGACAGCGGCAGGGATTGGATCCGATGACGACGAT
AAGGAATTC**GATGATAATCATCGCGGCAAATTCTACAGCCGTATGACCTATAGCATCAGTGCGGTTGAATA**
TCTGGGTCTGGTGTCGAAATCTCTGATGGTCAAAGGCAATCGGTCACTGAAGAAATTTGGTTGGGCTGCGA
TTGATGGTGTAACGGCACCTTTTGCTCGCATCAAGAAACGCTCCGTTAGCAACAAGAAACTCTACTCTACC
CCGTATGACATTCTGCACCTGGATCATCCAGCGTTGCGTAATGGGAACAAACTTTCCGACTTAGAAGCCAG
TATCTCGCGTTTGGAAGAACGCCTTGCACAGTTAGAGAAACGTGGCATTGCCATTAGCGGAAACCACCAGA
AACAACCGGAAACTGCCGAGAAAGAAAAGAAAGAAATCAACGAAGAGAAACGCGCGATTCTCCGTATGCTG
GTGAATGAGAACAAACAGCTGCGCAAAATGGCAGAAAACGCTAGCCATCACCATCATCACCACTAACGGCC
G

sfGFP-His

MGSKGEELFTGVVPILVELDGDVNGHKFSVRGEGEGDATNGKLTLKFICTTGKLPVPWPTLVTTLTYGVQC
FSRYPDHMKQHDFFKSAMPEGYVQERTISFKDDGTYKTRAEVKFEGDTLVNRIELKGIDFKEDGNILGHKL
EYNFNSHNVYITADKQKNGIKANFKIRHNVEDGSVQLADHYQQNTPIGDGPVLLPDNHYLSTQSVLSKDPN
EKRDHMVLLEFVTAAGIGSDDDDKEFASHHHHHH

CCATGGGCAGCAAGGGTGAGGAACTATTCACGGGCGTAGTTCCAATTCTCGTAGAGCTGGACGGGGATGTC
AACGGCCACAAATTTTCTGTGCGCGGGGAGGGGGAGGGGGATGCTACCAACGGCAAATTGACTTTGAAATT
TATCTGCACCACTGGTAAACTGCCTGTGCCTTGGCCGACGTTGGTTACGACCCTGACCTATGGAGTCCAAT
GTTTCTCGCGGTATCCGGATCACATGAAACAGCATGACTTCTTCAAGAGCGCAATGCCCGAGGGTTATGTG
CAAGAGCGCACTATCTCGTTTAAGGACGATGGCACTTATAAAACTCGCGCAGAAGTCAAGTTCGAGGGTGA
TACTTTAGTCAATCGTATAGAACTTAAAGGTATAGACTTCAAGGAAGATGGAAACATCCTGGGCCATAAAT
TAGAATATAATTTTAATAGCCACAATGTATACATTACCGCAGACAAACAAAAAAACGGTATAAAAGCTAAC
TTCAAAATTCGTCATAACGTGGAAGACGGATCGGTACAACTCGCCGACCATTACCAGCAAAACACTCCAAT
AGGTGATGGTCCGGTGCTGCTGCCGGATAACCACTATCTTTCTACTCAAAGTGTCCTAAGTAAAGACCCGA
ACGAAAAAAGAGATCATATGGTATTATTAGAATTTGTGACAGCGGCAGGGATTGGATCCGATGACGACGAT
AAGGAATTCGCTAGCCATCACCATCATCACCACTAACGGCCG

3. Recombinant protein expression

3.1. Methods

The fusion proteins were recombinantly expressed in the cytoplasm of the *E. coli* strain BL21(DE3), using standard protocols. Briefly, the expression cultures were inoculated from starter cultures (OD_{600} = 0.1) and grown at 37 °C and 180 rpm. Once OD_{600} reached a value between 0.6 and 0.8, protein expression was induced with 1 mM isopropyl-β-D-thiogalactopyranoside. After continued growth for 3 h at 37 °C and 180 rpm, the culture was harvested by centrifugation (6000g, 15 min, 4 °C). For protein purification under native conditions, the pellet was resuspended in loading buffer (10 mM Tricine/HCl pH 8, 300 mM NaCl, 15 mM imidazole), containing a protease inhibitor cocktail (SIGMA*FAST*™ Protease Inhibitor Cocktail, EDTA-Free; Sigma Aldrich). The bacteria suspension was lysed with a high-pressure homogenizer (EmulsiFlex-B15; Avestin). The cell lysate was cleared via centrifugation (20000g, 1 h, 4 °C). The supernatant was passed through 0.45 µm and 0.2 µm filters and loaded onto Ni^{2+}-NTA columns (His GraviTrap™; GE Healthcare), equilibrated with loading buffer. Each column was washed with 5 column volumes of loading buffer, washing buffer I (10 mM Tricine/HCl pH 8, 500 mM NaCl, 15 mM imidazole) and washing buffer II (10 mM Tricine/HCl pH 8, 300 mM NaCl, 30 mM imidazole). The proteins were eluted using 5 column volumes of elution buffer (10 mM Tricine/HCl pH 8, 300 mM NaCl, 400 mM imidazole). For sfGFP-Mad11-His, immobilized metal ion affinity chromatography under

these conditions did not yield any protein in the eluted fraction. After increasing the pH of the above buffers to 8.8 a small amount of the protein could be obtained. For purification under denaturing conditions (His-Mad10trunc and Mad10trunc-His), each buffer contained 8 M urea. The eluted sfGFP fusion proteins were dialyzed against 20 mM Tris/HCl pH 8, 50 mM NaCl (12-14 kDa MWCO; Spectra/Por®; Spectrum Labs). The protein solutions were concentrated to at least 1 mg mL^{-1} via ultrafiltration (10 kDa MWCO; Amicon Ultra-15; Merck), aliquoted and stored at -80 °C until use. Protein concentrations were determined based on absorbance measurements at 280 nm. The respective extinction coefficients were calculated using ProtParam (https://web.expasy.org/protparam/) and are listed in Table S1.

3.2. SDS-PAGE

The purity of the obtained proteins was analyzed using sodium dodecyl sulfate polyacrylamide gel electrophoresis (SDS-PAGE). Electrophoresis was performed under reducing conditions, following standard protocols. Fig. S12 shows all sfGFP fusion proteins purified under native conditions, incl. the control protein sfGFP-His. Fig. S13 shows Mad10trunc-His and His-Mad10trunc, purified under native and denaturing conditions.

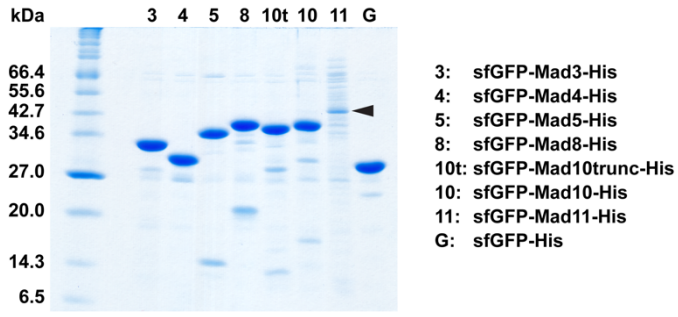

Figure S12. Reducing SDS-PAGE (12 %) showing all recombinantly expressed sfGFP fusion proteins after dialysis against 20 mM Tris/HCl pH 8, 50 mM NaCl. A total amount of 5 µg protein was loaded for each sample. With the exception of sfGFP-Mad11-His (black arrow), all proteins show sufficient purity for magnetite-binding assays.

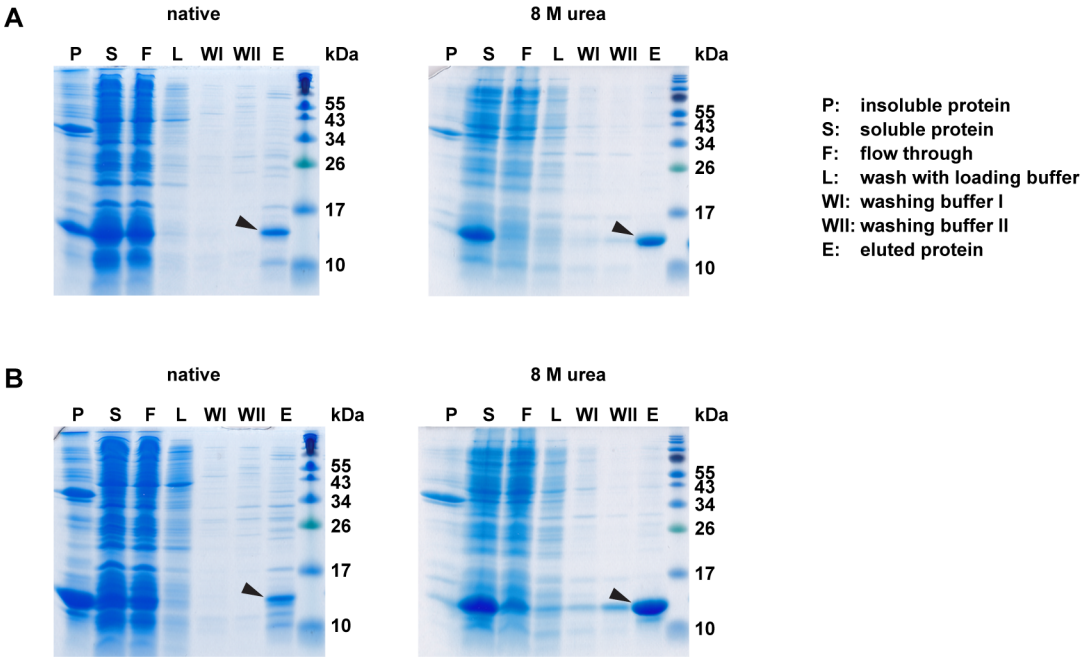

Figure S13. Reducing SDS-PAGE (18 %) showing the expression and purification of (A) His-Mad10trunc and (B) Mad10trunc-His. Both proteins were purified under native and denaturing conditions. The corresponding SDS-PAGE shows that only part of the protein was found in the soluble fraction when the cell pellet was dissolved and homogenized under native conditions. In addition, a certain amount of protein was observed in the flow through of the Ni^{2+}-NTA columns. When cell lysis and purification was performed under denaturing conditions (8 M urea) the protein was fully solubilized and bound to the Ni^{2+}-NTA column almost quantitatively. Taken together, these observations are a strong indication that both Mad10trunc proteins have a tendency to oligomerize or aggregate.

3.3. MALDI-TOF

The size of the purified proteins was further validated with mass spectrometry, using a matrix-assisted laser desorption/ionization time-of-flight (MALDI-TOF) spectrometer (Autoflex Speed; Bruker). The protein samples were desalted via ultrafiltration (3 kDa MWCO; Amicon Ultra-0.5; Merck), mixed with the matrix 2',4'-dihydroxyacetophenone (DHAP) and spotted onto the MALDI target plate. The measurement was performed in positive, long-pass mode (range 3000-53000 m/z or 10000-50000 m/z). A summary of the calculated and measured masses is provided in Table S1.

Table S1. Summary of the molecular properties of the purified proteins. The extinction coefficients and molecular weights were calculated with ProtParam. The measured masses were obtained from the peak of the singly charged species.

protein	extinction coefficient (M^{-1} cm^{-1})	calculated mass (Da)	measured mass (Da)
sfGFP-Mad3-His	17420	30447.91	30370
sfGFP-Mad4-His	22920	29911.32	29850
sfGFP-Mad5-His	24870	38747.19	38693
sfGFP-Mad8-His	28880	35737.21	35682
sfGFP-Mad10trunc-His	30370	40242.09	40054
sfGFP-Mad10-His	30370	40734.66	40687
sfGFP-Mad11-His	30370	44952.69	not determined
sfGFP-His	17420	27573.71	27518
His-Mad10trunc	12950	13945.73	not determined
Mad10trunc-His	12950	13884.65	not determined

The calculated masses of the sfGFP fusion proteins were corrected for the mass difference resulting from chromophore maturation (-20 Da).[9] In addition, the mass of the N-terminal Met was subtracted. The individual mass spectra of all proteins are shown in Fig. S14-S20. For the proteins sfGFP-Mad3-His, sfGFP-Mad4-His, sfGFP-Mad5-His, sfGFP-Mad8-His, sfGFP-Mad10trunc-His, sfGFP-Mad10-His and sfGFP-His, the relative difference between the calculated and measured masses is <0.5 %. No measurements were performed for sfGFP-Mad11-His because of its low purity.

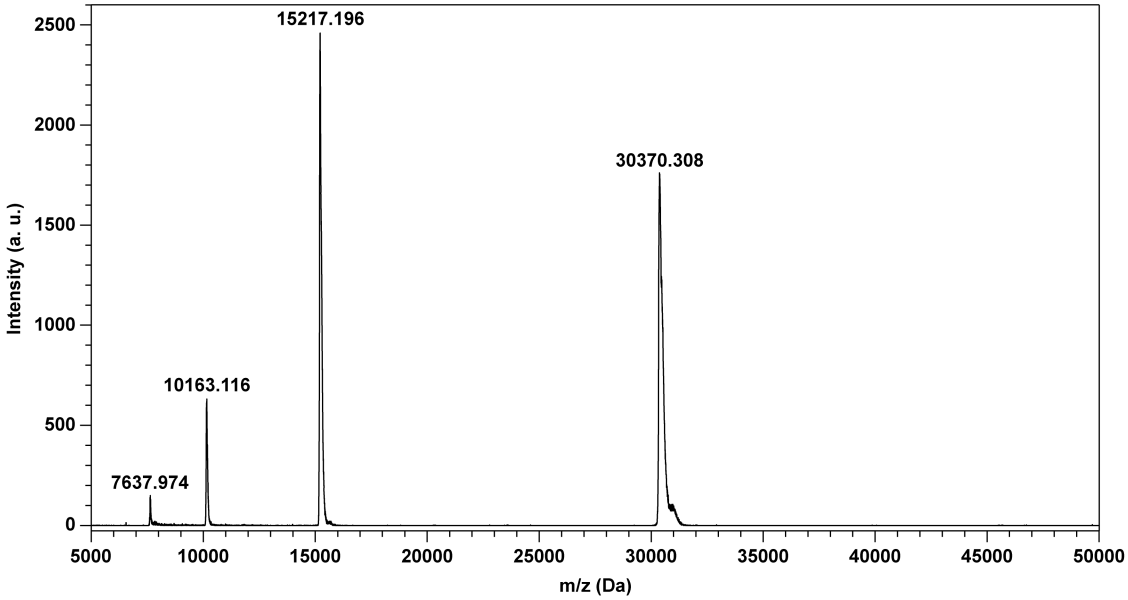

Figure S14. MALDI-TOF spectrum of **sfGFP-Mad3-His**. Calculated mass = 30447.91 Da; measured mass = 30370 Da.

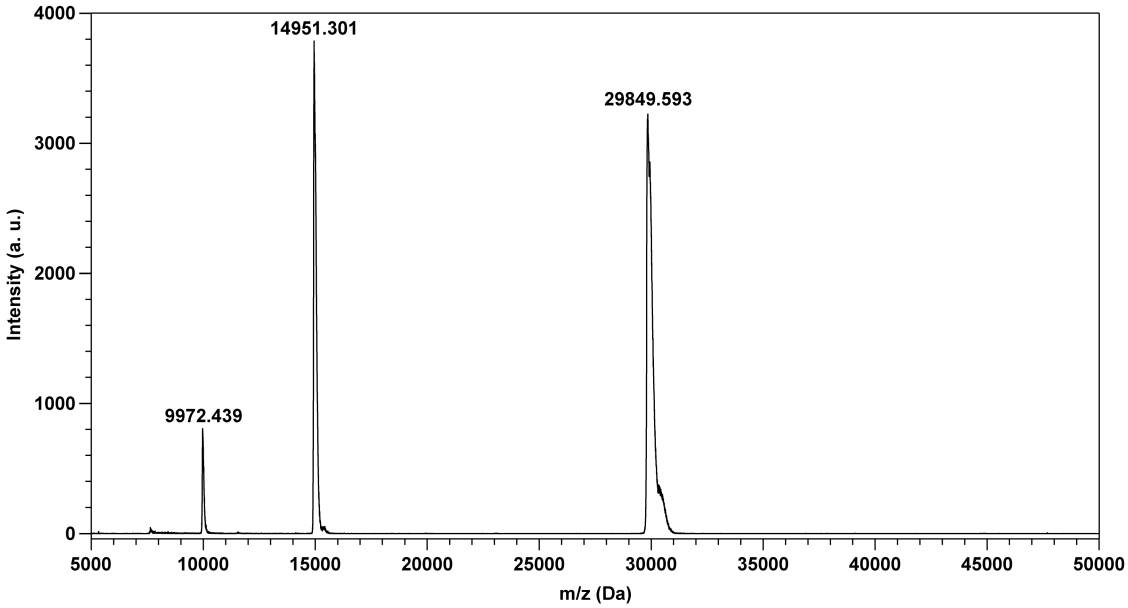

Figure S15. MALDI-TOF spectrum of **sfGFP-Mad4-His**. Calculated mass = 29911.32 Da; measured mass = 29850 Da.

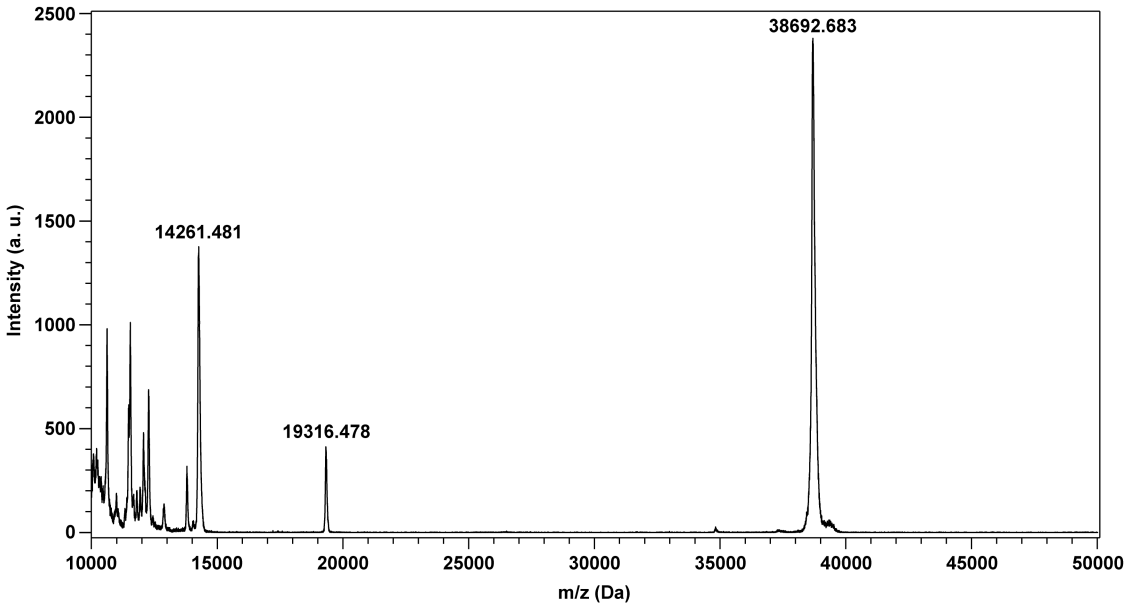

Figure S16. MALDI-TOF spectrum of **sfGFP-Mad5-His**. Calculated mass = 38747.19 Da; measured mass = 38693 Da.

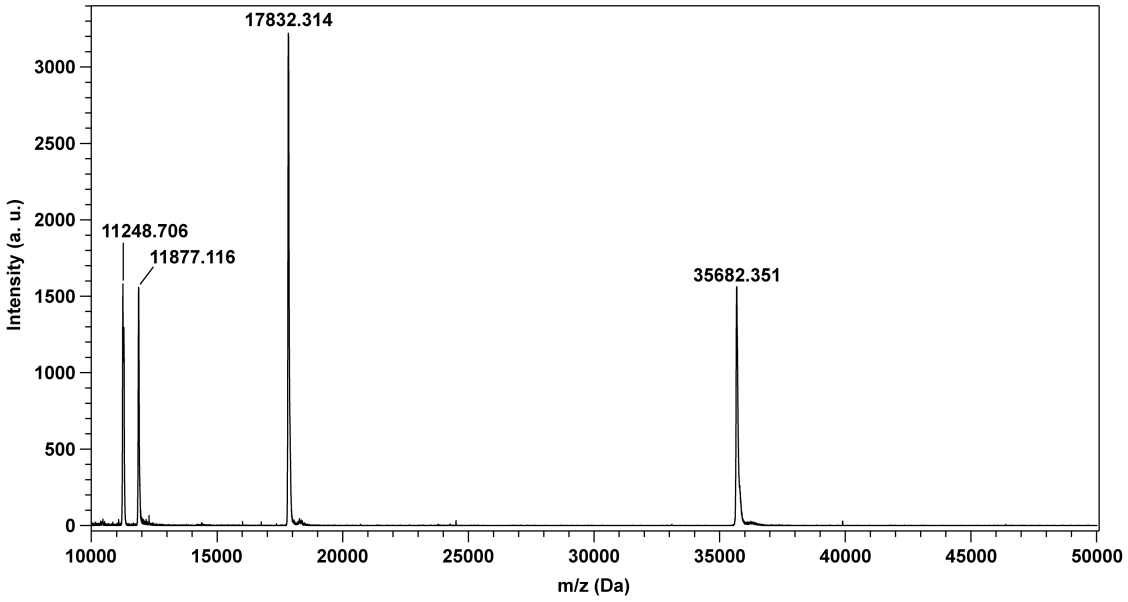

Figure S17. MALDI-TOF spectrum of **sfGFP-Mad8-His**. Calculated mass = 35737.21 Da; measured mass = 35682 Da.

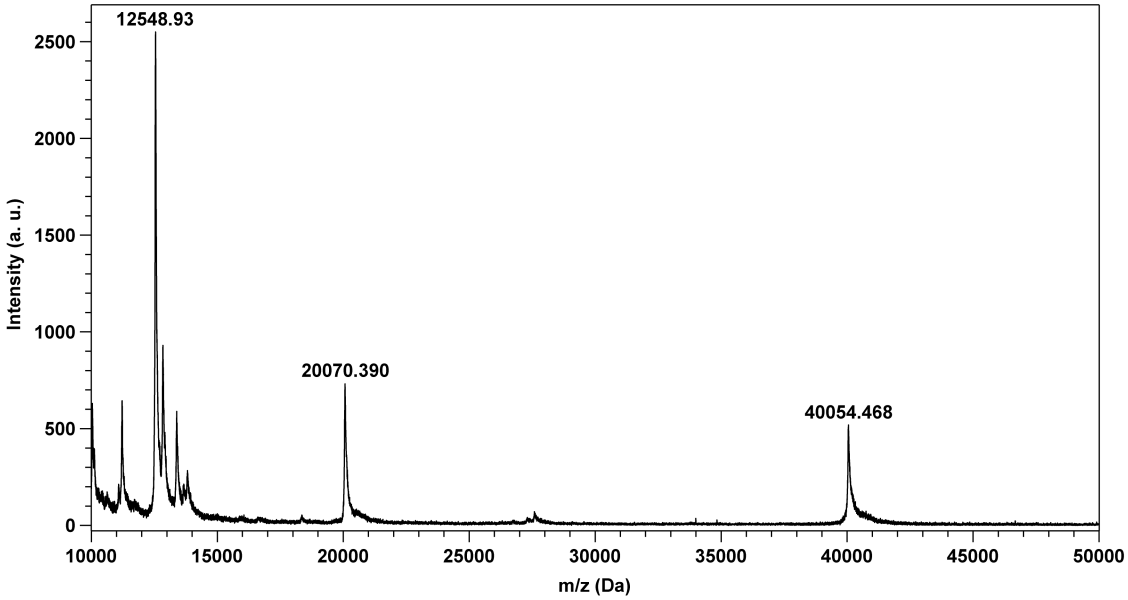

Figure S18. MALDI-TOF spectrum of **sfGFP-Mad10trunc-His**. Calculated mass = 40242.09 Da; measured mass = 40054 Da.

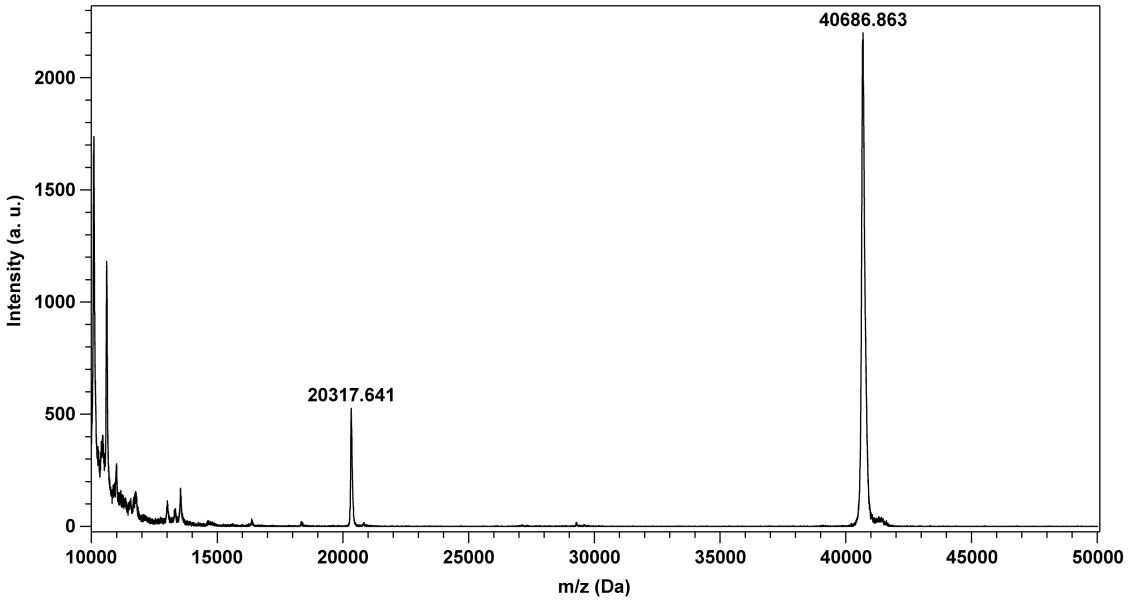

Figure S19. MALDI-TOF spectrum of **sfGFP-Mad10-His**. Calculated mass = 40734.66 Da; measured mass = 40687 Da.

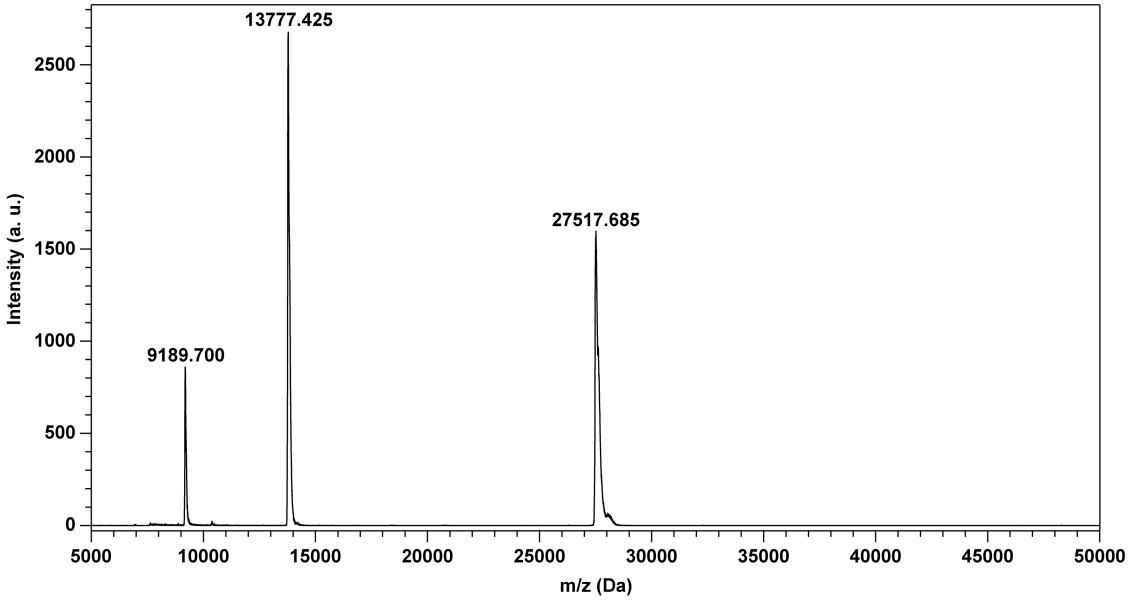

Figure S20. MALDI-TOF spectrum of **sfGFP-His**. Calculated mass = 27573.71 Da; measured mass = 27518 Da.

4. Quartz crystal microbalance with dissipation

4.1. Methods

Quartz crystal microbalance with dissipation (QCM-D) measurements were performed with the 4-channel system QSense Analyzer (Biolin Scientific), equipped with a peristaltic pump (Ismatec) and Tygon® tubing (diameter 0.64 mm; Ismatec). Commercially available sensor chips with a magnetite coating were obtained from LOT Quantum Design. Before starting the measurements, the sensors were cleaned using ultrapure water and dried with nitrogen. Then, the magnetite sensor chips were inserted into the liquid chamber and rinsed with ultrapure water and phosphate-buffered saline (PBS; 10 mM Na_2HPO_4/1.8 mM KH_2PO_4 pH 7.4, 137 mM NaCl, 2.7 mM KCl) until a stable baseline was obtained. Subsequently, the protein solution (diluted to 1 µM in PBS) was flushed through the liquid chamber at a flow rate of 25 µL min^{-1} to allow the proteins to bind to the magnetite surface. To observe protein dissociation from the surface, the sensor chips were further flushed with buffer for at least 4 h. After the experiment, the sensor chips were rinsed with water, dried with nitrogen and cleaned in an UV/ozone cleaner (ProCleaner; Bioforce Nanosciences) for 10 min.

4.2. Screening for magnetite binding

The binding of the sfGFP-Mad fusion proteins to the magnetite surface was screened in three independent experiments. The resulting frequency and dissipation data are shown in Fig. S21-S27.

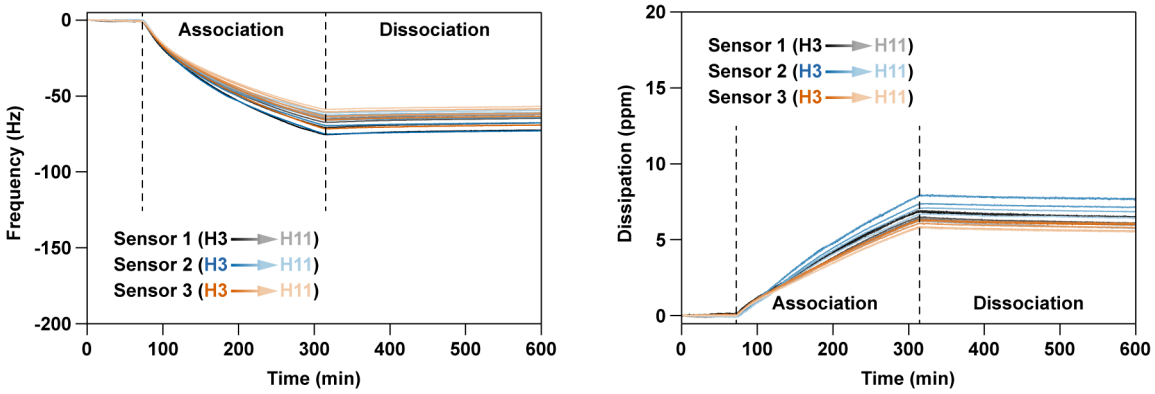

Figure S21. QCM-D-based magnetite-binding test for **sfGFP-Mad3-His**. The plots show the association (PBS + 1 µM protein) and dissociation (PBS) phases for both the frequency and dissipation signals. For each sensor surface, the harmonics (H) 3, 5, 7, 9 and 11 are plotted.

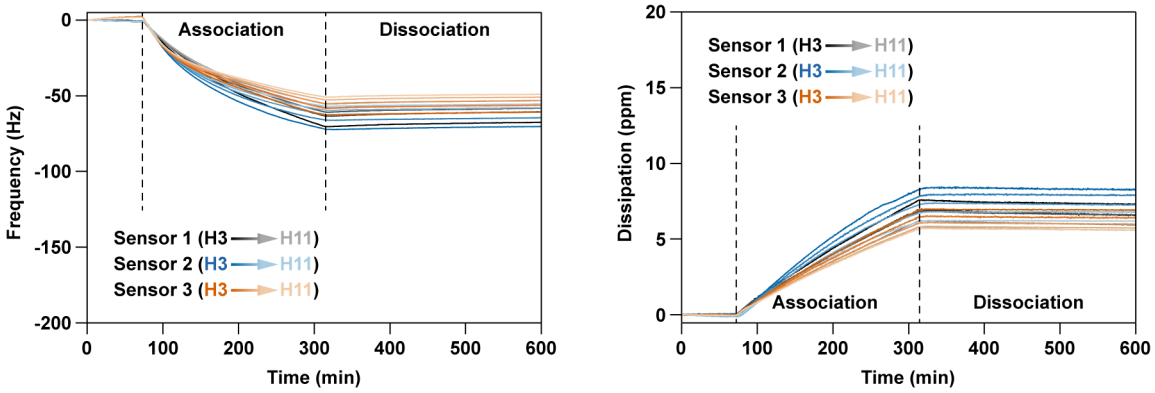

Figure S22. QCM-D-based magnetite-binding test for **sfGFP-Mad4-His**. The plots show the association (PBS + 1 µM protein) and dissociation (PBS) phases for both the frequency and dissipation signals. For each sensor surface, the harmonics (H) 3, 5, 7, 9 and 11 are plotted.

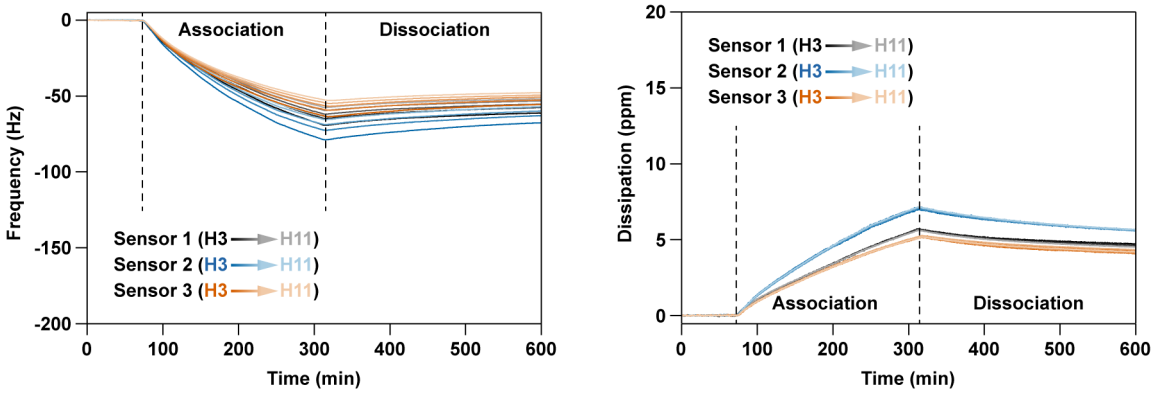

Figure S23. QCM-D-based magnetite-binding test for **sfGFP-Mad5-His**. The plots show the association (PBS + 1 µM protein) and dissociation (PBS) phases for both the frequency and dissipation signals. For each sensor surface, the harmonics (H) 3, 5, 7, 9 and 11 are plotted.

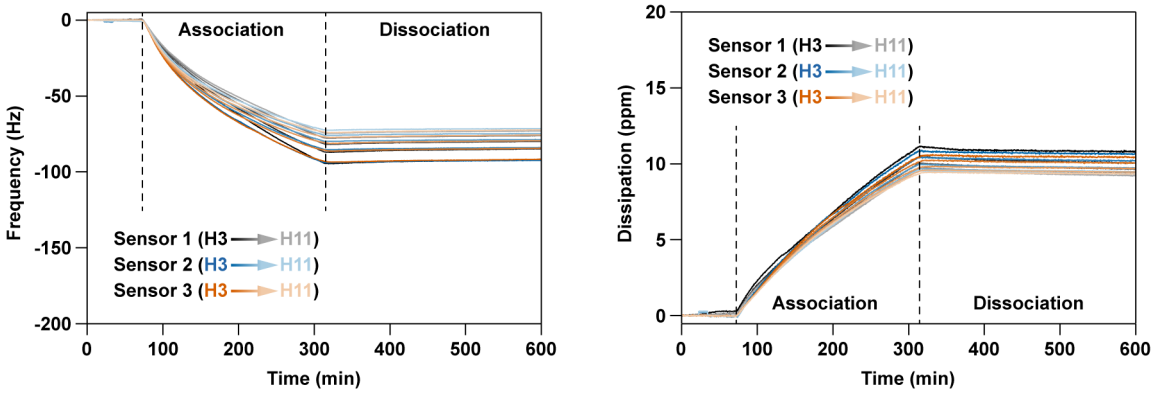

Figure S24. QCM-D-based magnetite-binding test for **sfGFP-Mad8-His**. The plots show the association (PBS + 1 µM protein) and dissociation (PBS) phases for both the frequency and dissipation signals. For each sensor surface, the harmonics (H) 3, 5, 7, 9 and 11 are plotted.

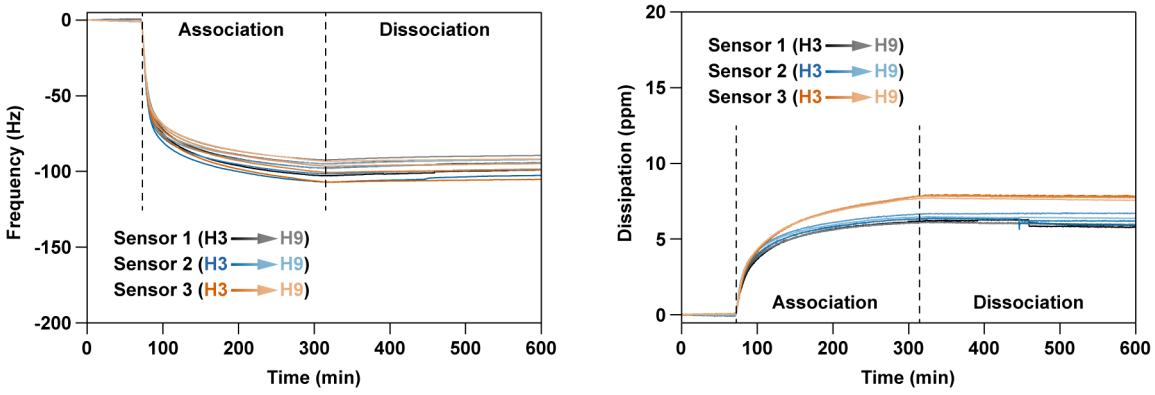

Figure S25. QCM-D-based magnetite-binding test for **sfGFP-Mad10-His**. The plots show the association (PBS + 1 µM protein) and dissociation (PBS) phases for both the frequency and dissipation signals. For each sensor surface, the harmonics (H) 3, 5, 7 and 9 are plotted.

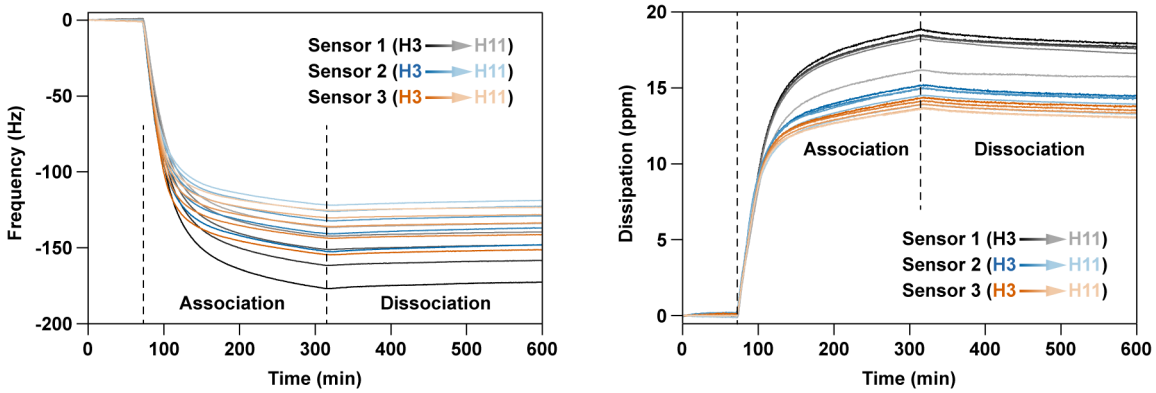

Figure S26. QCM-D-based magnetite-binding test for **sfGFP-Mad11-His**. The plots show the association (PBS + 1 µM protein) and dissociation (PBS) phases for both the frequency and dissipation signals. For each sensor surface, the harmonics (H) 3, 5, 7, 9 and 11 are plotted.

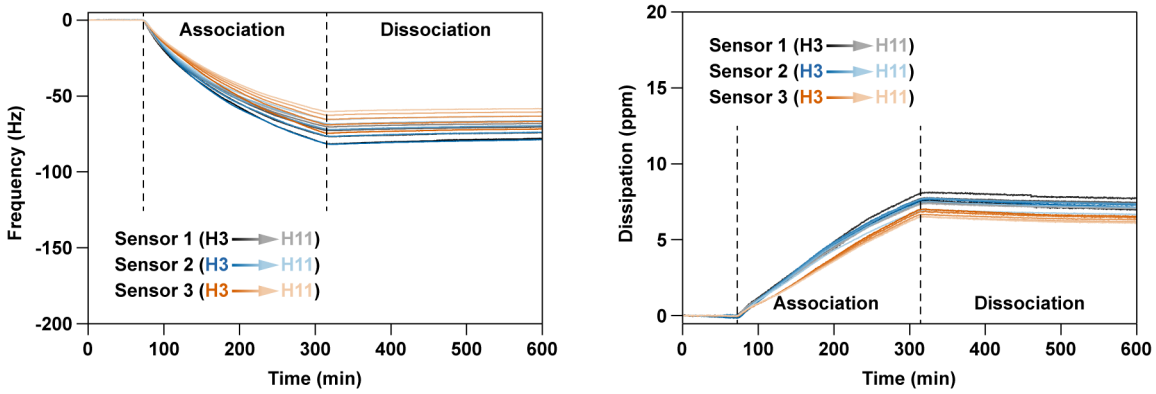

Figure S27. QCM-D-based magnetite-binding test for **sfGFP-His**. The plots show the association (PBS + 1 µM protein) and dissociation (PBS) phases for both the frequency and dissipation signals. For each sensor surface, the harmonics (H) 3, 5, 7, 9 and 11 are plotted.

4.3. Specificity analysis (sfGFP-Mad10-His vs. sfGFP-His)

To validate that the binding of sfGFP-Mad10-His to the sensor surface originates from a specific interaction between Mad10 and magnetite, a competitive binding experiment was performed (Fig. S28). One magnetite sensor chip was first exposed to sfGFP-Mad10-His and then incubated with sfGFP-His, while the order was reversed for a second sensor chip. If Mad10 does bind to the magnetite surface specifically, it is expected that the sfGFP-Mad10-His fusion protein displaces non-specifically bound sfGFP-His. Indeed, the strong change in the frequency and dissipation signals upon addition of

sfGPF-Mad10-His to the sfGFP-His coated surface supports this hypothesis. In contrast, no change in the frequency and dissipation signals was observed when sfGFP-His was flushed over the sensor surface that was previously exposed to sfGPF-Mad10-His. In combination, these results provide strong support for a specific interaction between Mad10 and magnetite.

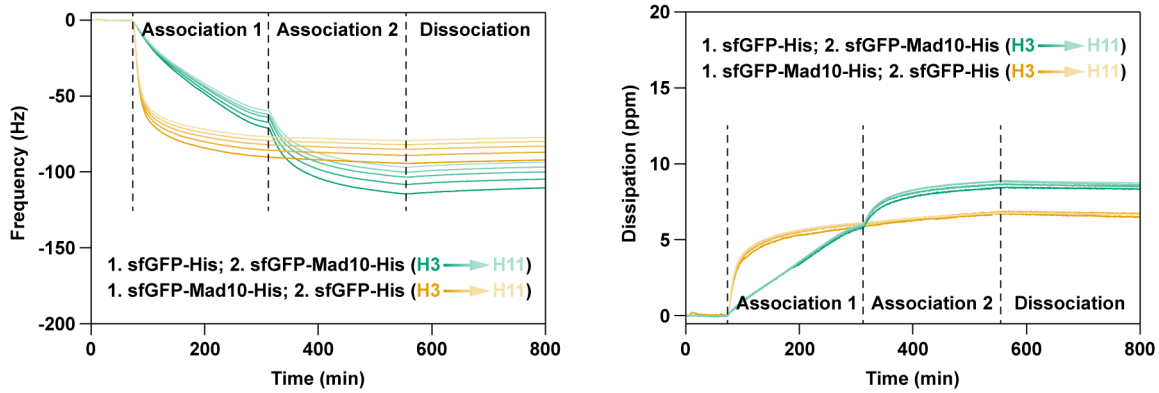

Figure S28. Competition QCM-D experiment to test for the specific binding of sfGFP-Mad10His to the magnetite surface. Shown are the frequency and dissipation signals of the sensor surface first exposed to sfGFP-Mad10-His (association phase 1) and then to sfGFP-His (association phase 2) and the sensor surface where the two proteins were added in reverse order. During each association phase, the protein concentration was 1 µM in PBS. During the subsequent dissociation phase, the sensor surface was rinsed with PBS. Shown are the harmonics (H) 3, 5, 7, 9 and 11.

4.4. Specificity analysis (mixture of Mad proteins)

The Mad10-magnetite interaction was further probed after mixing sfGFP-Mad10-His with sfGFP-Mad3-His, sfGFP-Mad4-His, sfGFP-Mad5-His and sfGFP-Mad8-His (each 1 µM in PBS). As a control, the same mixture of Mad fusion proteins without sfGFP-Mad10-His was used. This experiment is expected to further validate the specific interaction between Mad10 and magnetite. The results show that sfGFP-Mad10-His binds to the magnetite surface faster than the control mixture of the other Mad proteins. During the association phase, the frequency and dissipation signals further reach plateau values that are below the final values reached for the control mixture. Just as in the competition experiment with sfGFP-His (Fig. S28), this suggests that the surface is blocked against non-specific adsorption of other proteins once sfGFP-Mad10-His is bound.

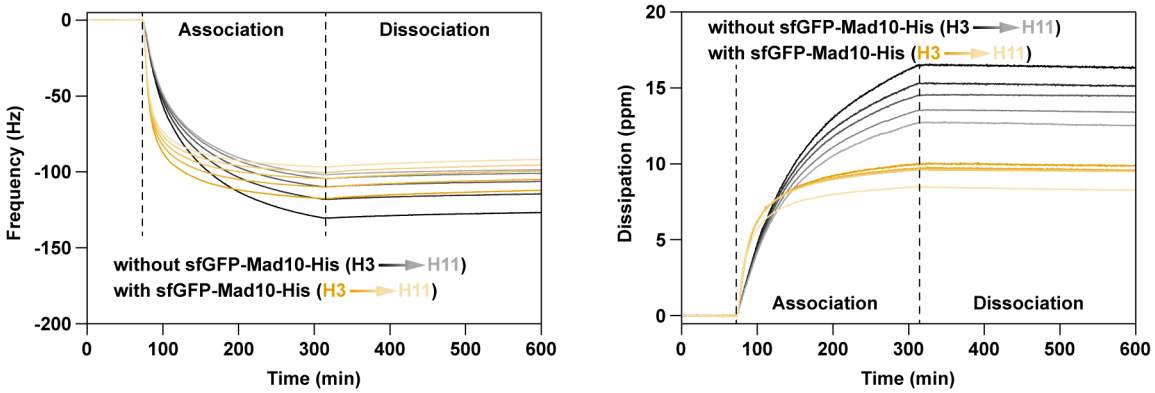

Figure S29. QCM-D experiment to test for the specific binding of sfGFP-Mad10His to the magnetite surface from a mixture of Mad proteins. Shown are the frequency and dissipation signals of mixtures with and without sfGFP-Mad10-His. The other proteins in the mixture were sfGFP-Mad3-His, sfGFP-Mad4-His, sfGFP-Mad5-His and sfGFP-Mad8-His. The concentration of each protein during the association phase was 1 µM in PBS. During the subsequent dissociation phase, the sensor surface was rinsed with PBS. Shown are the harmonics (H) 3, 5, 7, 9 and 11.

5. Co-precipitation of magnetite nanoparticles

5.1. Co-precipitation method

For magnetite nanoparticle (MNP) synthesis, co-precipitation experiments were performed according to the literature.[10] Within the 50 mL reaction vessel, the reaction took place under controlled conditions. The temperature was kept at 25 °C, using a thermostat (Julaba F12) and a thermostat jacket. The pH was constantly monitored with a Biotrode electrode and kept at 9.0 ± 0.4. A titration device (Methrom AG), consisting of a dosing unit (Dosimat 805) and a titration unit (Titrino 888), was used to add NaOH solution (0.1 M). Before starting a reaction, all solutions were flushed with nitrogen and a nitrogen atmosphere was maintained during the reaction. The reaction vessel was filled with 10 mL of ultrapure water, adjusted to pH 9.0 ± 0.4. For reactions performed in the presence of protein (sfGFP-Mad10-His, sfGFP-Mad10trunc-His, sfGFP-His), the respective protein was added to the reaction to obtain a final concentration of 0.5 µM. Before adding the protein, the protein solution was desalted via ultrafiltration (10 kDa MWCO; Amicon Ultra-0.5; Merck). Iron ions were added in a total concentration of 0.1 M and a ratio of Fe(II)/Fe(III) = 1:2. The Fe(II)/Fe(III) solution contained iron (II)

chloride tetrahydrate (33 mM) and iron (III) chloride hexahydrate (67 mM), dissolved in ultrapure water. The Fe(II)/Fe(III) solution was added to the reaction vessel dropwise (1 µL min^{-1}) under continuous stirring. Particle synthesis was performed for 6 h and a sample (100 µL) was taken every hour (3-4 independent experiments). The resulting nanoparticles were stored under argon at 4 °C.

5.2. Transmission electron microscopy

The resulting nanoparticles were visualized with transmission electron microscopy (TEM). For preparing TEM samples, a small amount of the nanoparticle suspension (10 µL) was dropped onto Parafilm. Subsequently, a copper grid coated with a carbon film was placed on top of the droplet. After the carbon film was in contact with the droplet for 10 min at room temperature, it was separated from the droplet and the remaining liquid was removed with absorbent paper. The grid was placed onto Parafilm with the carbon site facing up for 30 min to ensure complete drying. The samples were imaged with a Zeiss 912 Omega transmission electron microscope. An acceleration voltage of 120 kV was used to obtain low-magnification bright field images (Fig. S30). The images show nanoparticles with a large size distribution. The MNPs synthesized in the absence and presence of protein do not show any difference in particle shape (Fig. S30).

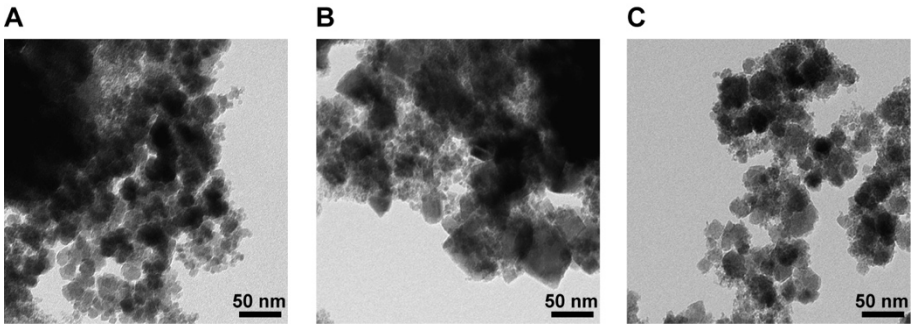

Figure S30. TEM micrographs showing nanoparticles co-precipitated in the absence and presence of protein. A) Co-precipitation performed in the absence of protein. B) Co-precipitation performed in the presence 0.5 µM sfGFP-His. C) Co-precipitation performed in the presence 0.5 µM sfGFP-Mad10trunc-His. All reactions were performed at 25 °C and pH = 9.0 ± 0.4 and the samples shown represent the 6-hour time point.

5.3. X-ray diffraction

The aggregation of the nanoparticles in the TEM samples prohibits an accurate analysis of their size. Instead, X-ray diffraction (XRD) was performed at the μ-Spot beam line of the BESSY II synchrotron (Helmholtz-Zentrum Berlin).[11] XRD further allows for the analysis of the crystal structure of the nanoparticles and thus provides information if the formed nanoparticles are magnetite. Samples for XRD were prepared in the following way. A Kapton film (Breitlander GmbH) was placed into a sample holder, which contained 54 holes covered by the film. For each hole, 10 μL of the nanoparticle suspension were dropped onto the film. Further, an α-quartz standard (SiO_2; 1878a; NIST) was added and used as the XRD standard. The suspensions dried on the film and the sample holder was mounted in a sample-detector distance of ~180 mm. The samples were measured with a 100 μm beam in transmission mode. The wavelength was set to 0.826 Å, using a Si111 monochromator. An Eiger X 9M detector (Dectris) was used. The exposure time was between 10-180 s, depending on the signal intensity.

For data analysis, the DPDAK software was used.[12] First, the exact sample-to-detector distance was calculated, using the α-quartz standard. The position of the magnetite (311) peak was used for further lattice parameter calculations and the XRD diffractogram was compared with a magnetite reference provided by the German Federal Institute for Materials Research and Testing (BAM). The instrumental peak broadening and the full-width-at-half-maximum (FWHM) of the magnetite (311) peak were determined by fitting the (311) peak with a pseudo-Voigt function. The mean crystallite diameter was determined using the Scherrer equation and the corrected FWHM.[13] The resulting particle diameter values, obtained from 3-4 independent co-precipitation reactions, are reported in Table S2. At the early time points, no MNPs were detected in some samples and mean values are thus not reported.

Table S2. Summary of MNP diameters. The data represents 3-4 independent co-precipitation reactions, performed in the presence of 0.5 µM of the respective protein, as well as a protein-free control. Samples were taken every hour and analysed with XRD. The error represents the standard error of the mean (SEM). Samples where no particles were found are indicated as "—". No mean value was calculated when less than 3 diameter values were available per condition.

1 h	**control**	**sfGFP-His**	**sfGFP-Mad10-His**	**sfGFP-Mad10trunc-His**
1	—	18.21	22.13	15.75
2	21.05	14.90	—	16.52
3	—	19.06	—	20.11
4	16.35	18.10		21.07
mean	**—**	**17.57**	**—**	**18.36**
SEM	**—**	**0.91**	**—**	**1.31**

2 h	**control**	**sfGFP-His**	**sfGFP-Mad10-His**	**sfGFP-Mad10trunc-His**
1	25.67	21.44	29.04	29.26
2	27.54	21.36	23.08	20.97
3	24.87	22.62	—	25.77
4		22.32		25.40
mean	**26.03**	**21.93**	**—**	**25.35**
SEM	**0.79**	**0.32**	**—**	**1.70**

3 h	**control**	**sfGFP-His**	**sfGFP-Mad10-His**	**sfGFP-Mad10trunc-His**
1	27.88	18.17	32.39	30.31
2	32.79	24.16	26.38	23.91
3	28.32	25.66	31.01	30.67
4		25.68		30.35
mean	**29.66**	**23.42**	**29.93**	**28.81**
SEM	**1.57**	**1.79**	**1.82**	**1.64**

4 h	**control**	**sfGFP-His**	**sfGFP-Mad10-His**	**sfGFP-Mad10trunc-His**
1	32.79	25.62	34.00	32.19
2	33.67	25.50	29.26	27.01
3	32.27	26.97	33.26	33.37
4		27.13		32.36
mean	**32.91**	**26.31**	**32.17**	**31.23**
SEM	**0.41**	**0.43**	**1.47**	**1.43**

5 h	control	sfGFP-His	sfGFP-Mad10-His	sfGFP-Mad10trunc-His
1	33.23	26.21	34.97	30.16
2	31.62	25.61	30.82	28.97
3	35.49	29.95	35.44	34.48
4		29.67		34.59
mean	**33.44**	**27.86**	**33.74**	**32.05**
SEM	**1.12**	**1.13**	**1.47**	**1.46**

6 h	control	sfGFP-His	sfGFP-Mad10-His	sfGFP-Mad10trunc-His
1	36.84	28.26	33.81	30.77
2	31.07	26.92	31.05	29.39
3	35.77	29.73	32.89	33.36
4		30.57		35.09
mean	**34.56**	**28.87**	**32.58**	**32.15**
SEM	**1.77**	**0.81**	**0.81**	**1.28**

5.4. Fluorescence microscopy

Fluorescence microscopy was used to verify that the sfGFP fusion protein had bound to the MNPs during the co-precipitation reaction (Fig. S31). For fluorescence microscopy (DMI8-CS, Leica), the MNPs synthesized in the presence of sfGFP-His or sfGFP-Mad10trunc-His were washed three times with ultrapure water adjusted to pH~9 with NaOH. The resulting MNP suspension was dropped onto a microscope slide and a coverslip was placed on top of the suspension. The inverted samples were measured in bright field mode and with a filter set optimized for GFP (excitation filter: 470/40 nm; dichroic mirror: 500 nm; emission filter: 525/50 nm).

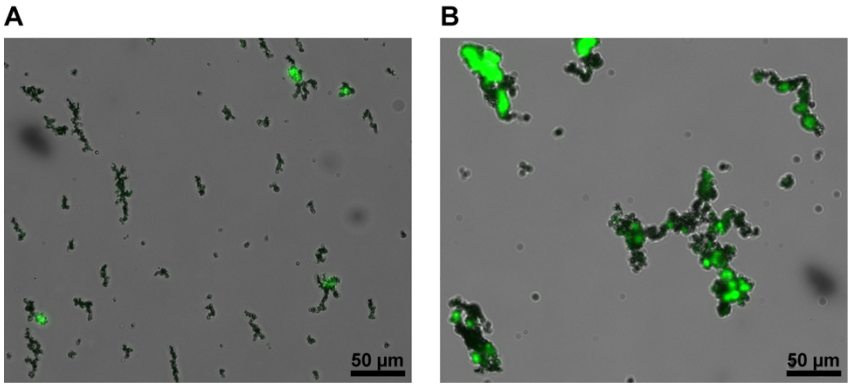

Figure S31. MNPs synthesized in the presence of (A) 1 µM sfGFP-His and (B) 1 µM sfGFP-Mad10trunc-His. After synthesis, the particles were washed 3x with ultrapure water adjusted to pH~9 using NaOH. The co-precipitation reaction was performed at 25 °C and pH = 9.0 ± 0.4. A 0.1 M Fe solution was added with a rate of 1 µL min^{-1}.

6. Magnetite-binding mechanism of Mad10

To better understand the type of interaction between Mad10 with the magnetite surface, the charge distribution was analyzed for the tertiary structure predicted with Raptor-X (Fig. S32).

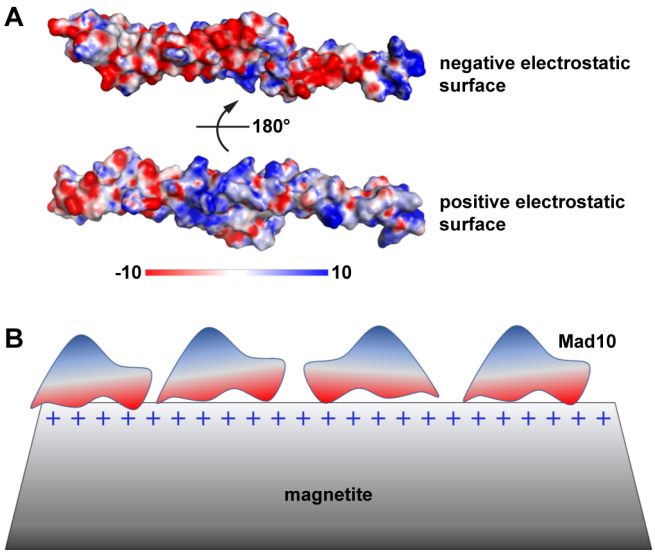

Figure S32. Mad10-magnetite interaction mode. (A) Mad10 surface coloured by electrostatic potential. Red and blue represent negative and positive potentials, respectively. The bar represents the electrostatic scale in arbitrary units. The images were calculated and prepared with PyMOL. (B) Suggested binding mechanism. The negatively charged residues and oxygen atoms of polar amino acids are predicted to interact directly with positively charged iron on the magnetite surface.

Similar to the magnetite-binding protein MamC, Mad10 shows a stretch of negatively charged amino acids on one side of the protein while the other side shows a net positive charge. This suggests that the negatively charged face may interact with the positively charged magnetite surface. The positively charged face may help to orient the protein or allow for interactions with phospholipids in the magnetosome membrane.

7. References

1. J. J. Almagro Armenteros, K. D. Tsirigos, C. K. Sønderby, T. N. Petersen, O. Winther, S. Brunak, G. von Heijne and H. Nielsen, *Nat. Biotechnol.*, 2019, **37**, 420.
2. A. Krogh, B. Larsson, G. von Heijne and E. L. Sonnhammer, *J. Mol. Biol.*, 2001, **305**, 567.
3. M. Källberg, H. Wang, S. Wang, J. Peng, Z. Wang, H. Lu and J. Xu, *Nat. Protoc.*, 2012, **7**, 1511.
4. a) A. Roy, A. Kucukural and Y. Zhang, *Nat. Protoc.*, 2010, **5**, 725; b) J. Yang, R. Yan, A. Roy, D. Xu, J. Poisson and Y. Zhang, *Nat. Methods*, 2015, **12**, 7; c) J. Yang and Y. Zhang, *Nucleic Acids Res.*, 2015, **43**, W174.
5. M. I. Siponen, G. Adryanczyk, N. Ginet, P. Arnoux and D. Pignol, *Biochem. Soc. Trans.*, 2012, **40**, 1319.
6. A. Pohl, F. Berger, R. M. A. Sullan, C. Valverde-Tercedor, K. Freindl, N. Spiridis, C. T. Lefèvre, N. Menguy, S. Klumpp, K. G. Blank and D. Faivre, *Nano Lett.*, 2019, **19**, 8207.
7. J. D. Pédelacq, S. Cabantous, T. Tran, T. C. Terwilliger and G. S. Waldo, *Nat. Biotechnol.*, 2006, **24**, 79.
8. a) X. Li, G. Zhang, N. Ngo, X. Zhao, S. R. Kain and C. C. Huang, *J. Biol. Chem.*, 1997, **272**, 28545; b) H. K. Kim and B. K. Kaang, *Brain Res. Bull.*, 1998, **47**, 35.
9. L. Zhang, H. N. Patel, J. W. Lappe and R. M. Wachter, *J. Am. Chem. Soc.*, 2006, **128**, 4766.
10. J. Baumgartner, M. Antonietta Carillo, K. M. Eckes, P. Werner and D. Faivre, *Langmuir*, 2014, **30**, 2129.
11. O. Paris, C. Li, S. Siegel, G. Weseloh, F. Emmerling, H. Riesemeier, A. Erko and P. Fratzl, *J. Appl. Crystallogr.*, 2007, **40**, s466.

12. G. Benecke, W. Wagermaier, C. Li, M. Schwartzkopf, G. Flucke, R. Hoerth, I. Zizak, M. Burghammer, E. Metwalli, P. Müller-Buschbaum, M. Trebbin, S. Förster, O. Paris, S. V. Roth and P. Fratzl, *J. Appl. Crystallogr.*, 2014, **47**, 1797.
13. A. Fischer, M. Schmitz, B. Aichmayer, P. Fratzl and D. Faivre, *J. R. Soc. Interface*, 2011, **8**, 1011.